

Supporting Information

Synthesis, Biological Evaluation, and In Silico Studies of New Acetylcholinesterase Inhibitors Based on Quinoxaline Scaffold

Paptawan Suwanhom, Jirakrit Saetang, Pasarat Khongkow, Teerapat Nualnoi, Varomyalin Tipmanee and Luelak Lomlim

- Nuclear magnetic resonance spectra for the synthesized quinoxaline and its derivatives**
- IC₅₀ curves for the inhibition of *Hu*AChE and *eq*BChE by quinoxaline derivatives (3a-6c), tacrine and galanthamine**
- 2D Figure indicated interaction between synthesized compound and the amino acids at AChE binding site**

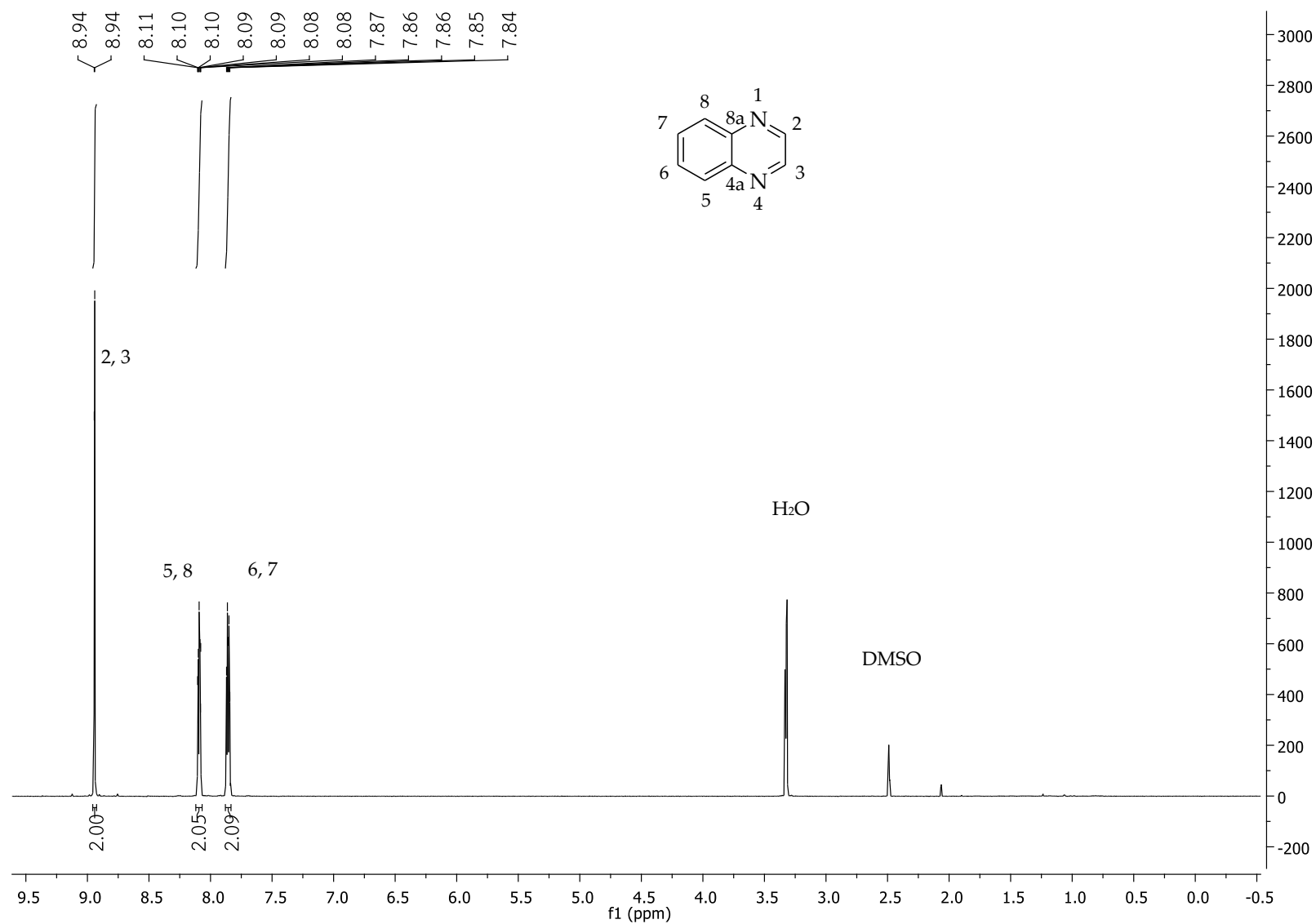


Figure 1. $^1\text{H-NMR}$ spectra of Quinoxaline (3a).

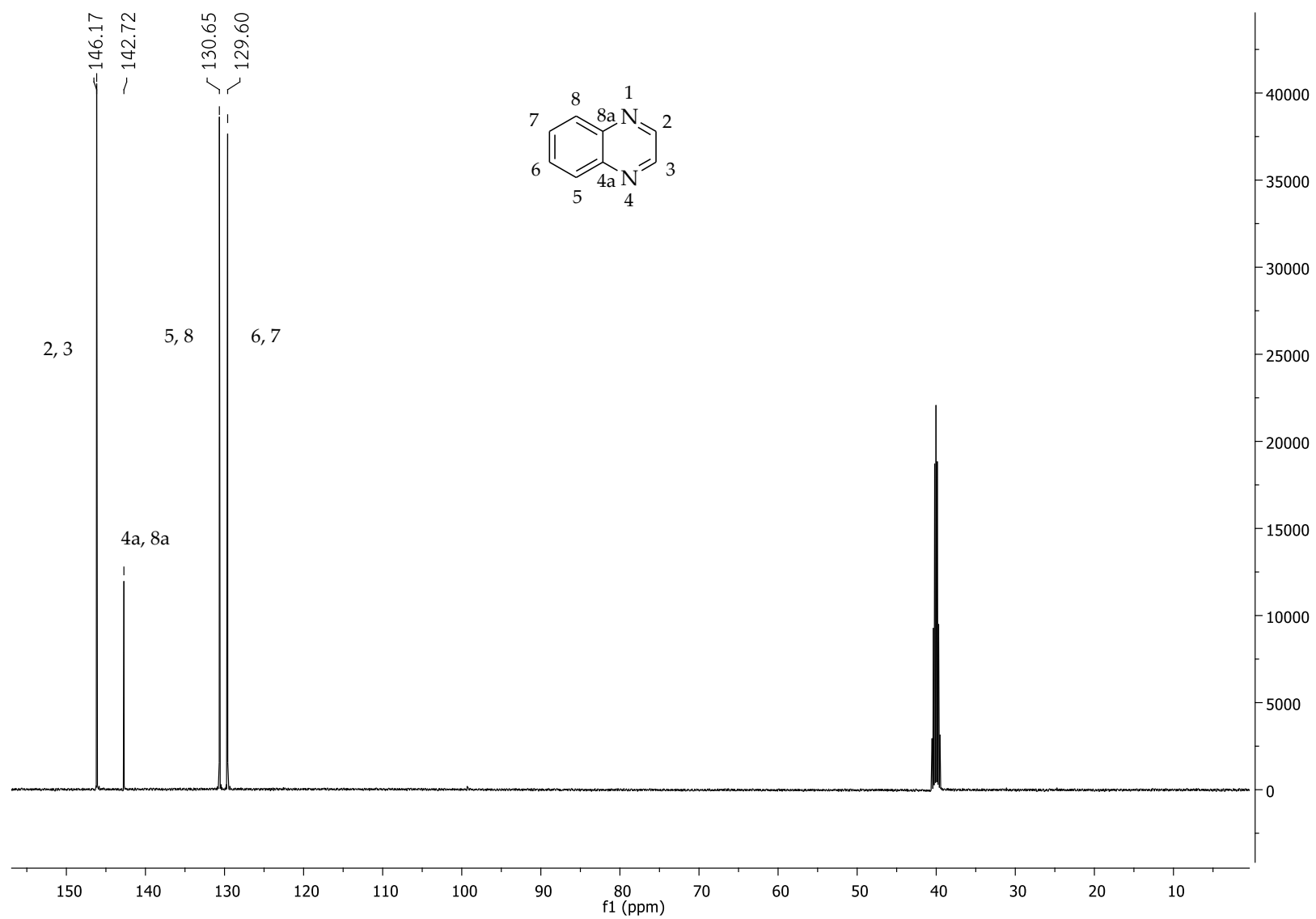


Figure 2. ^{13}C -NMR spectra of Quinoxaline (3a).

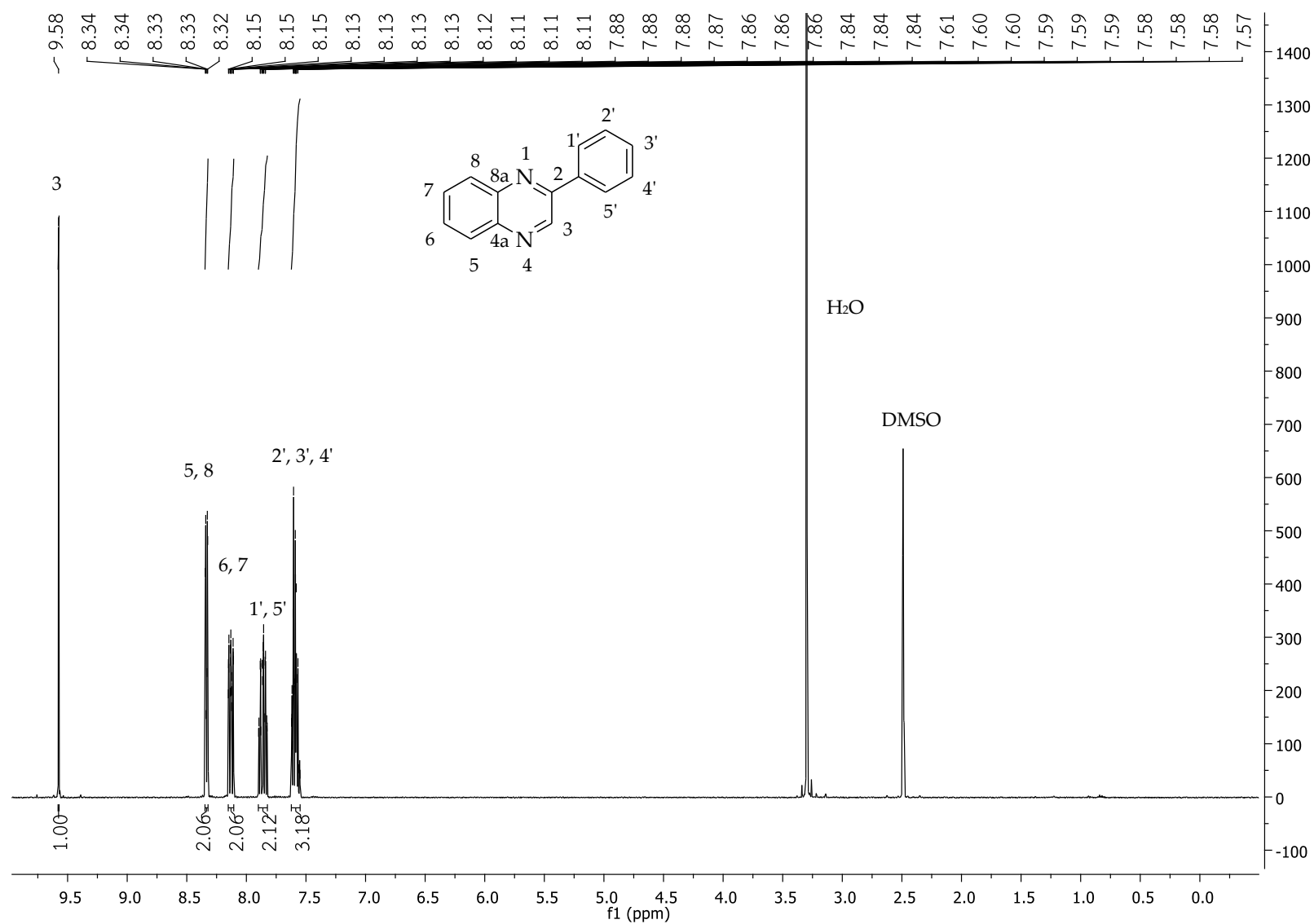


Figure 3. $^1\text{H-NMR}$ spectra of 2-Phenylquinoxaline (3b).

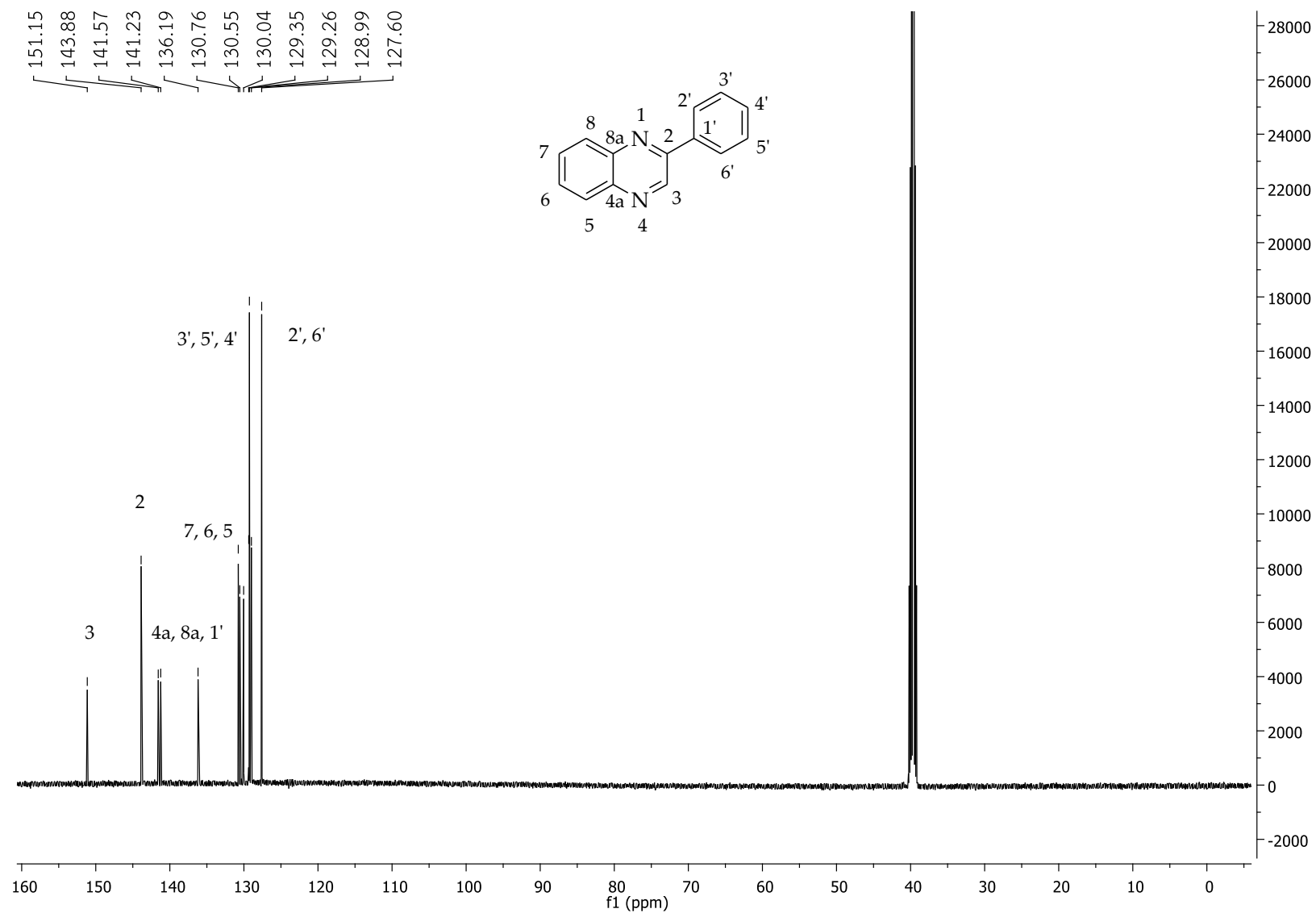


Figure 4. ^{13}C -NMR spectra of 2-Phenylquinoxaline (3b).

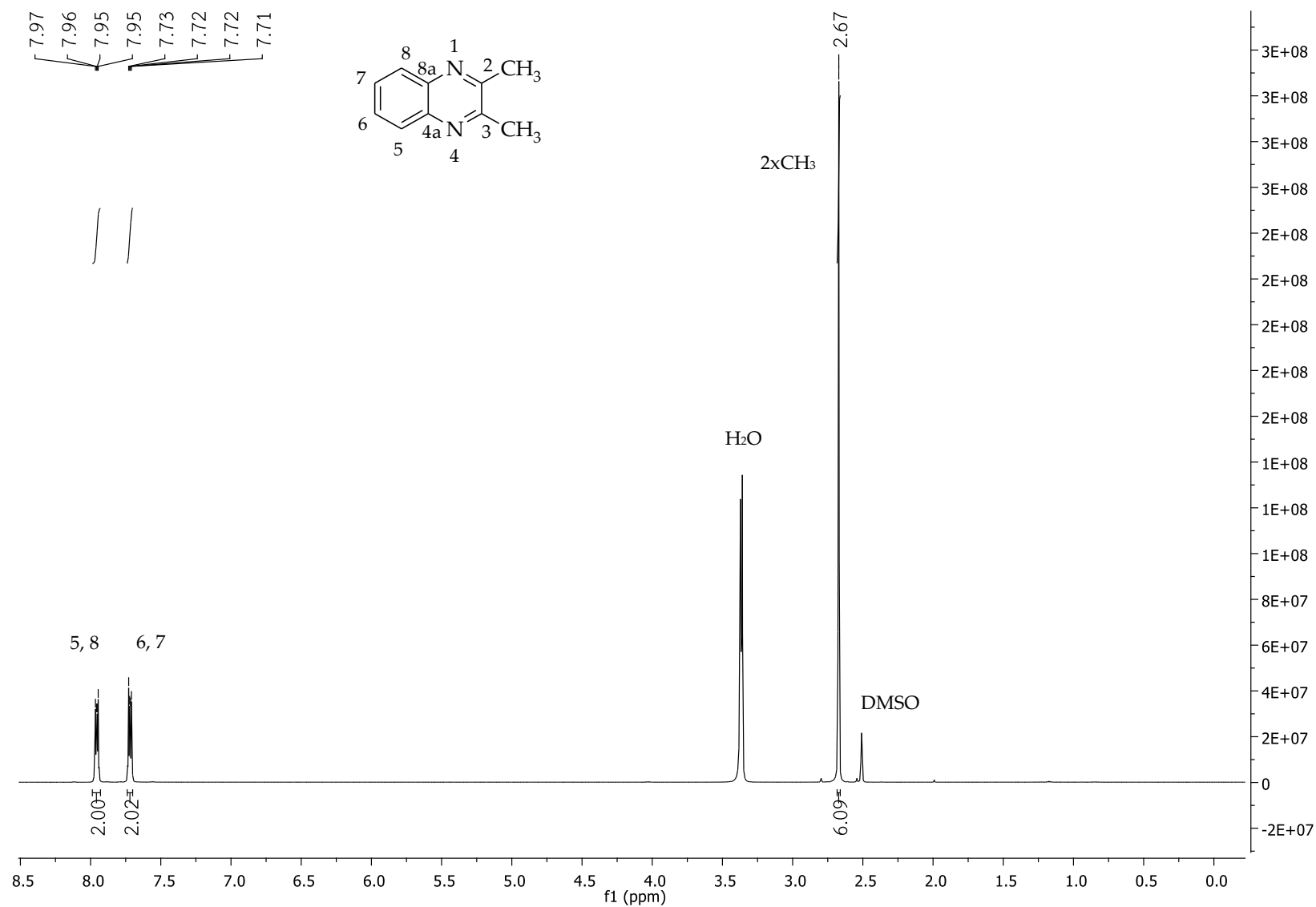


Figure 5. $^1\text{H-NMR}$ spectra of 2,3-Dimethylquinoxaline (3c).

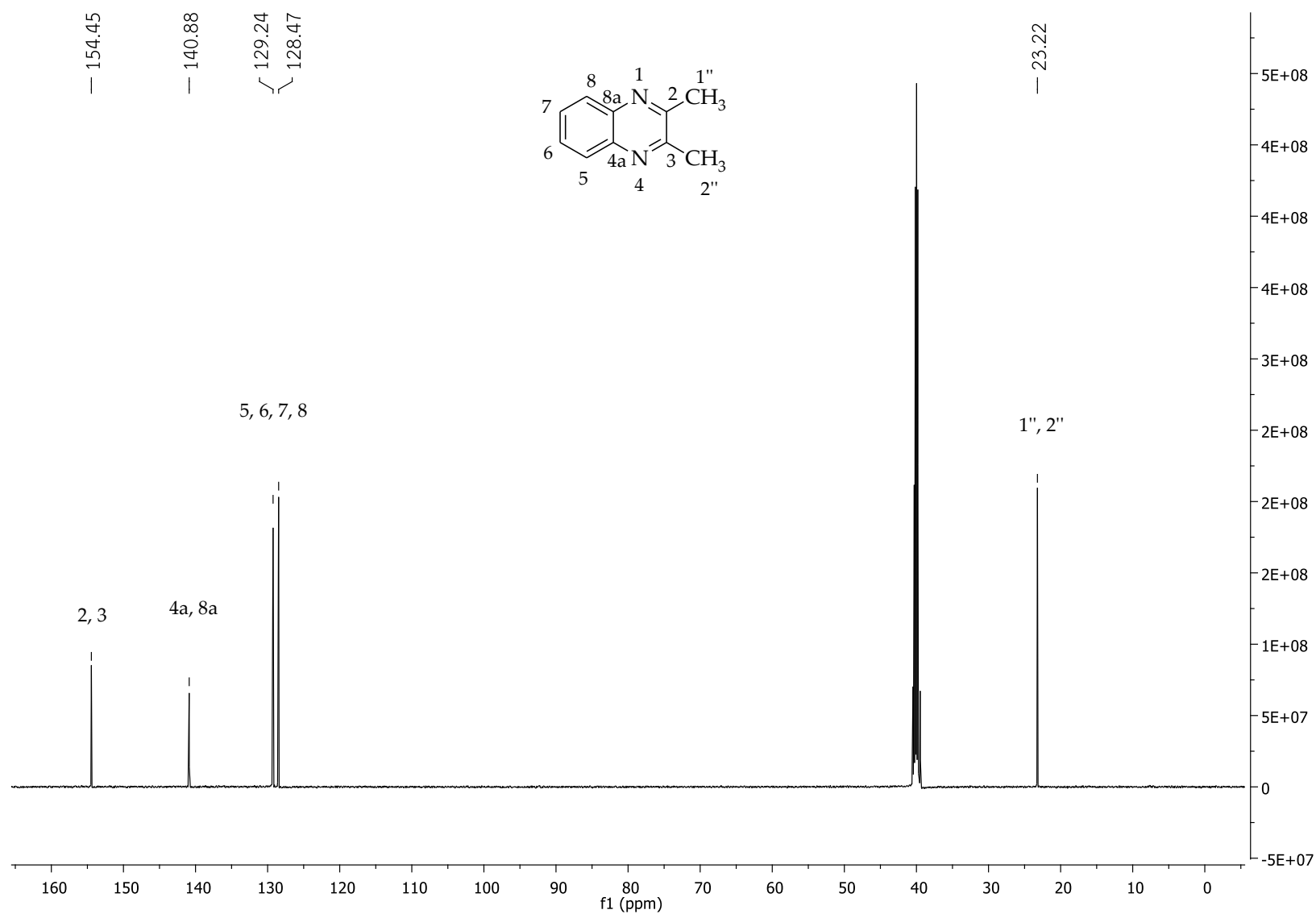


Figure 6. ^{13}C -NMR spectra of 2,3-Dimethylquinoxaline (3c).

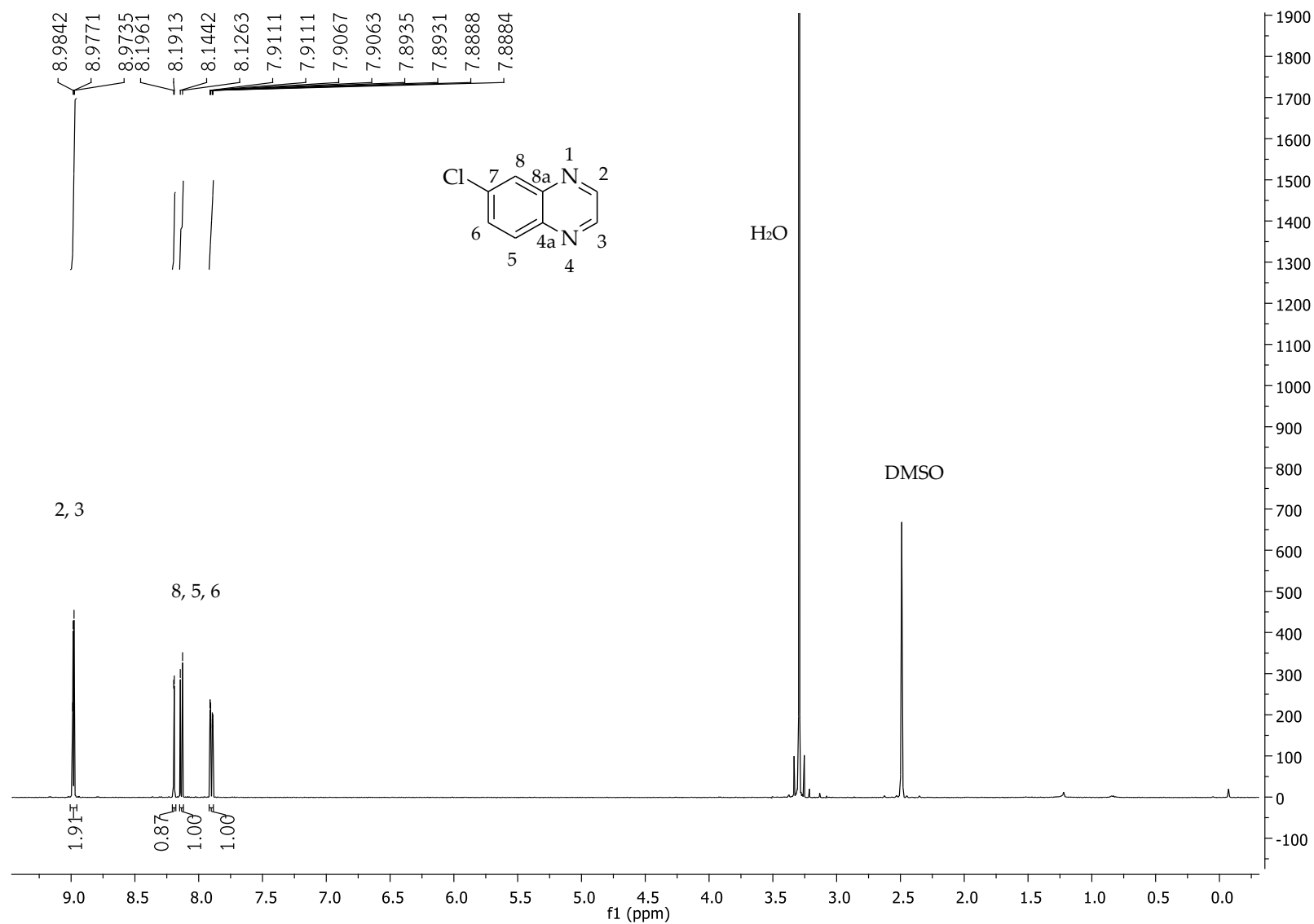


Figure 7. $^1\text{H-NMR}$ spectra of 6-Chloroquinoxaline (4a).

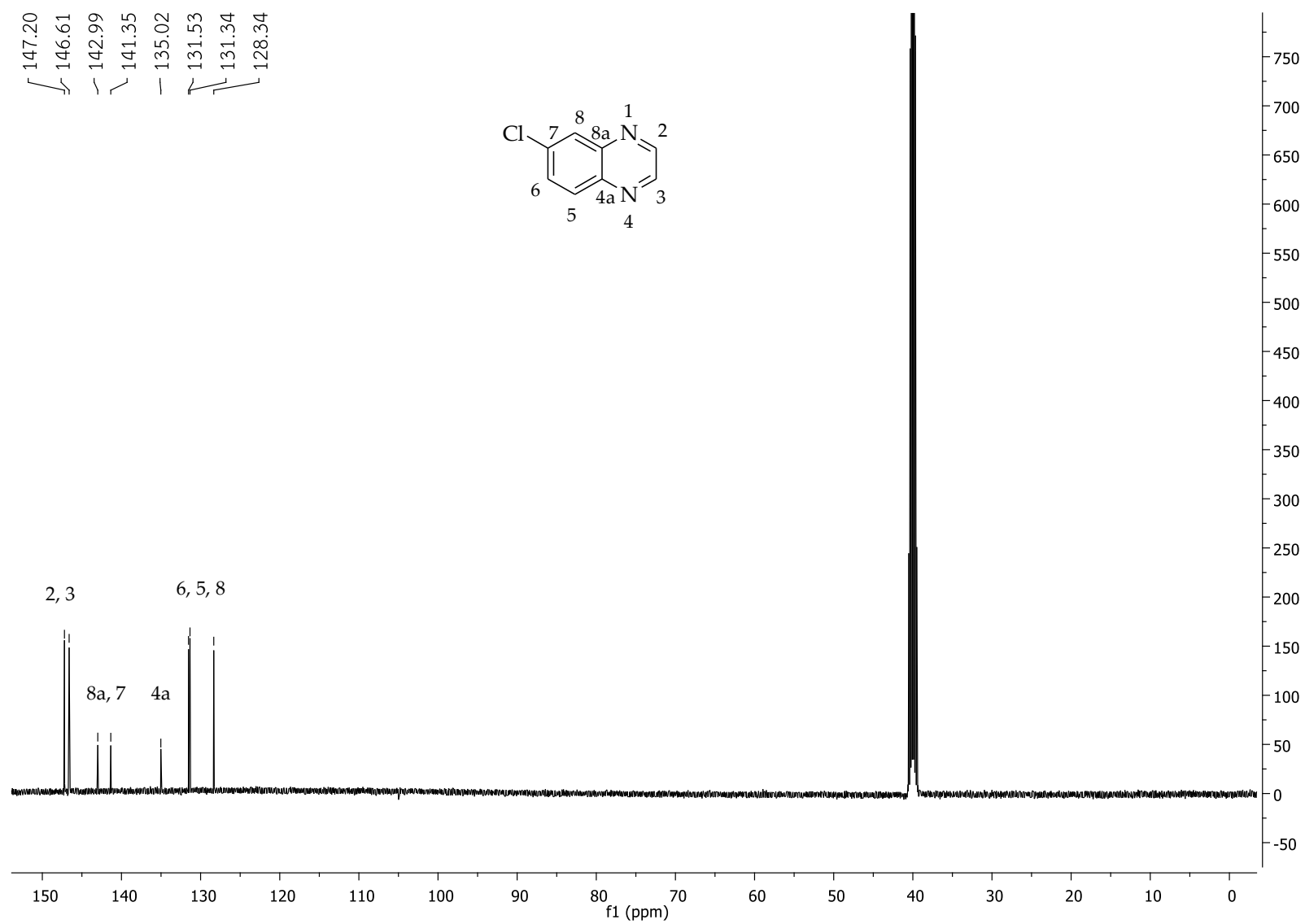


Figure 8. ^{13}C -NMR spectra of 6-Chloroquinoxaline (4a).

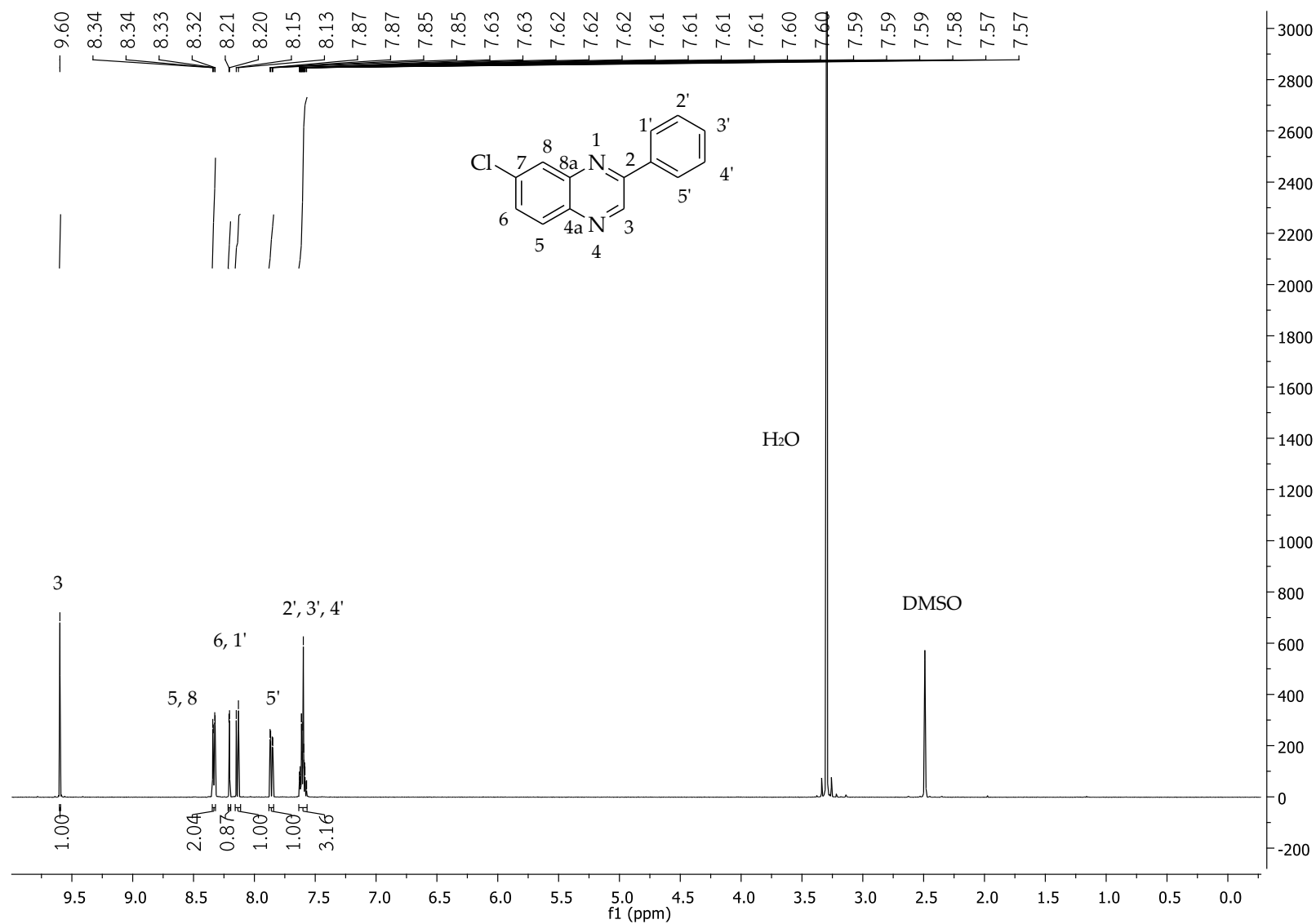


Figure 9. ¹H-NMR spectra of 7-Chloro-2-phenylquinoxaline (4b).

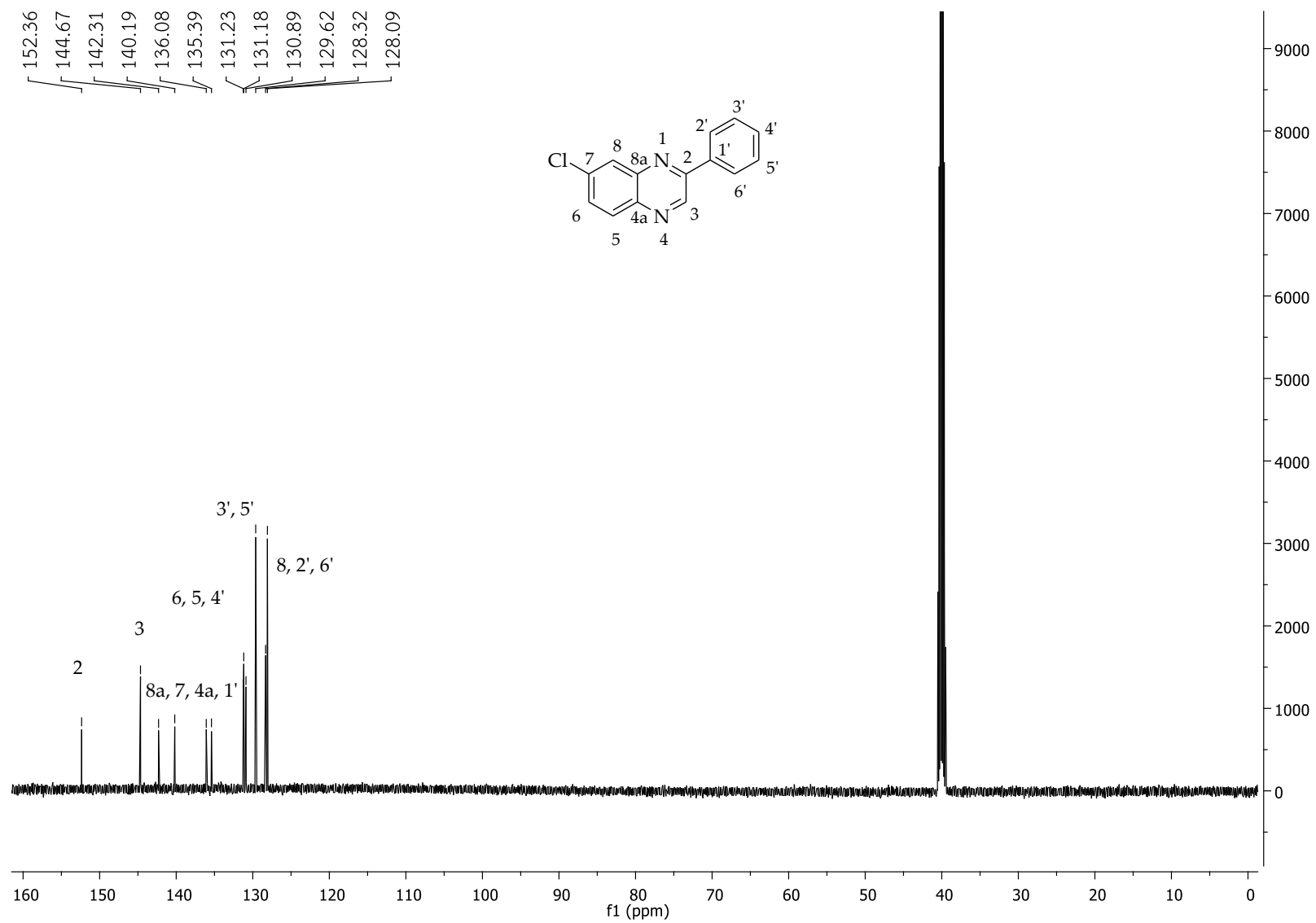


Figure 10. ^{13}C -NMR spectra of 7-Chloro-2-phenylquinoxaline (4b).

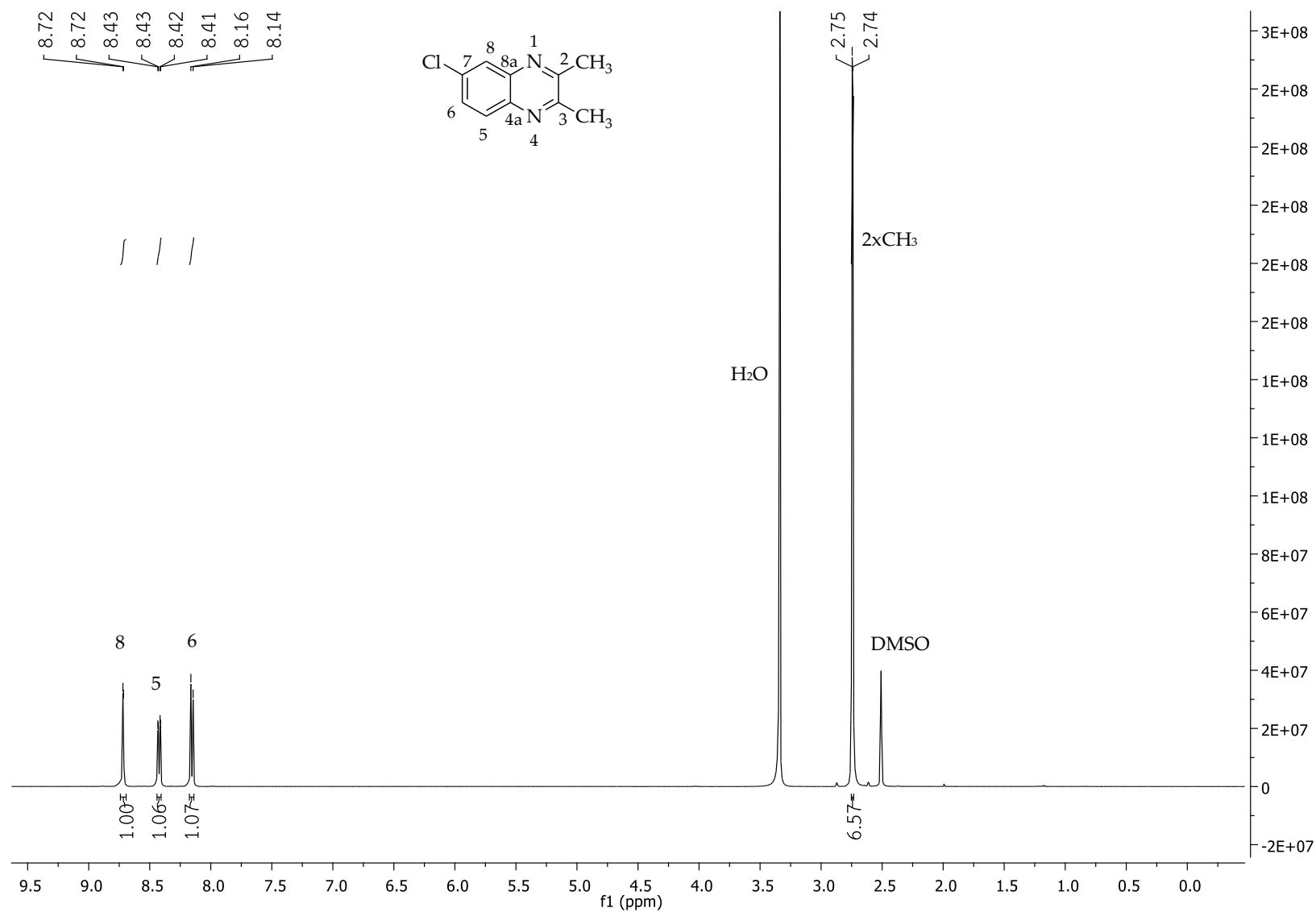


Figure 11. $^1\text{H-NMR}$ spectra of 6-chloro-2,3-dimethylquinoxaline (4c).

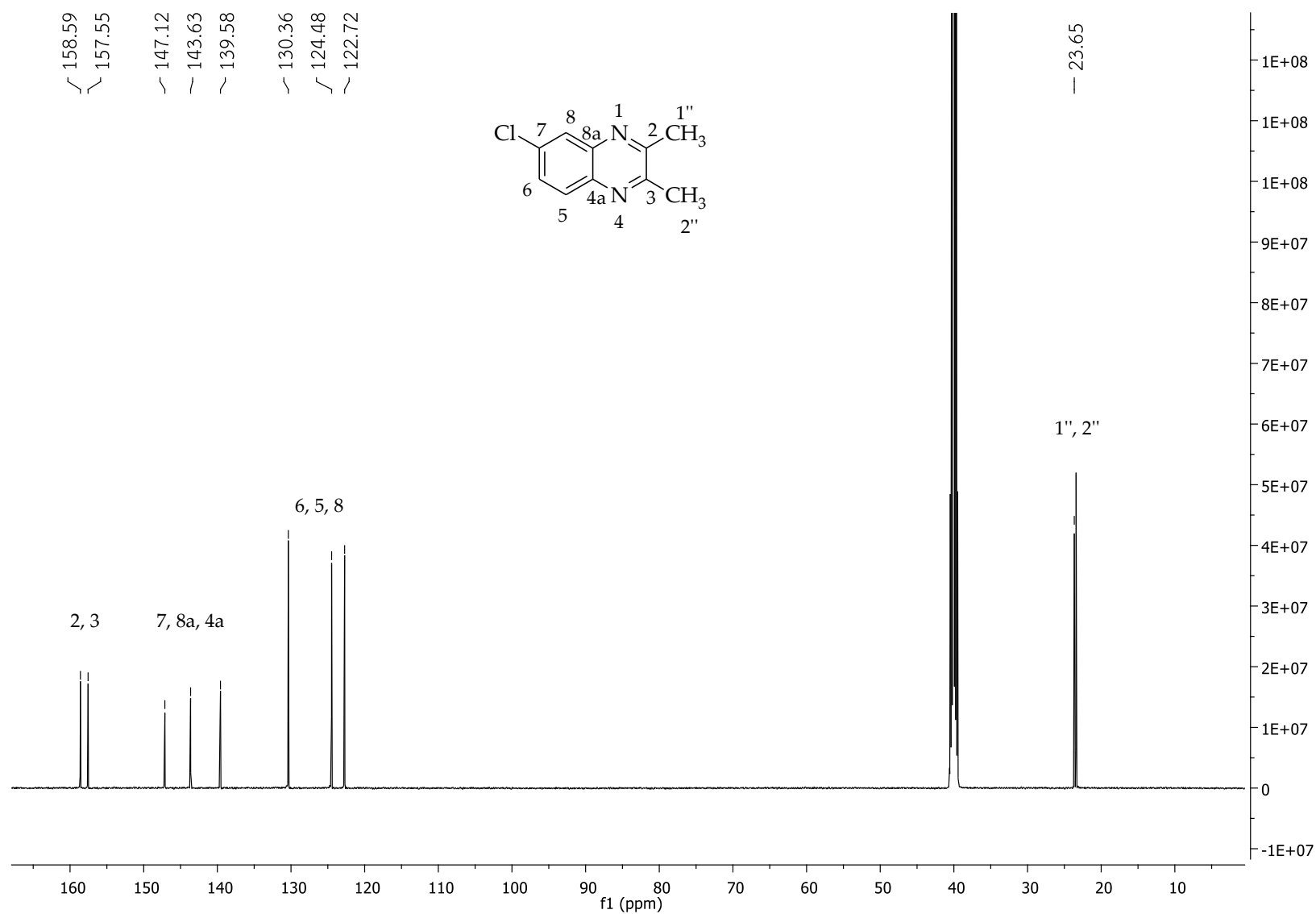


Figure 12. ¹³C-NMR spectra of 6-Chloro-2,3-dimethylquinoxaline (4c).

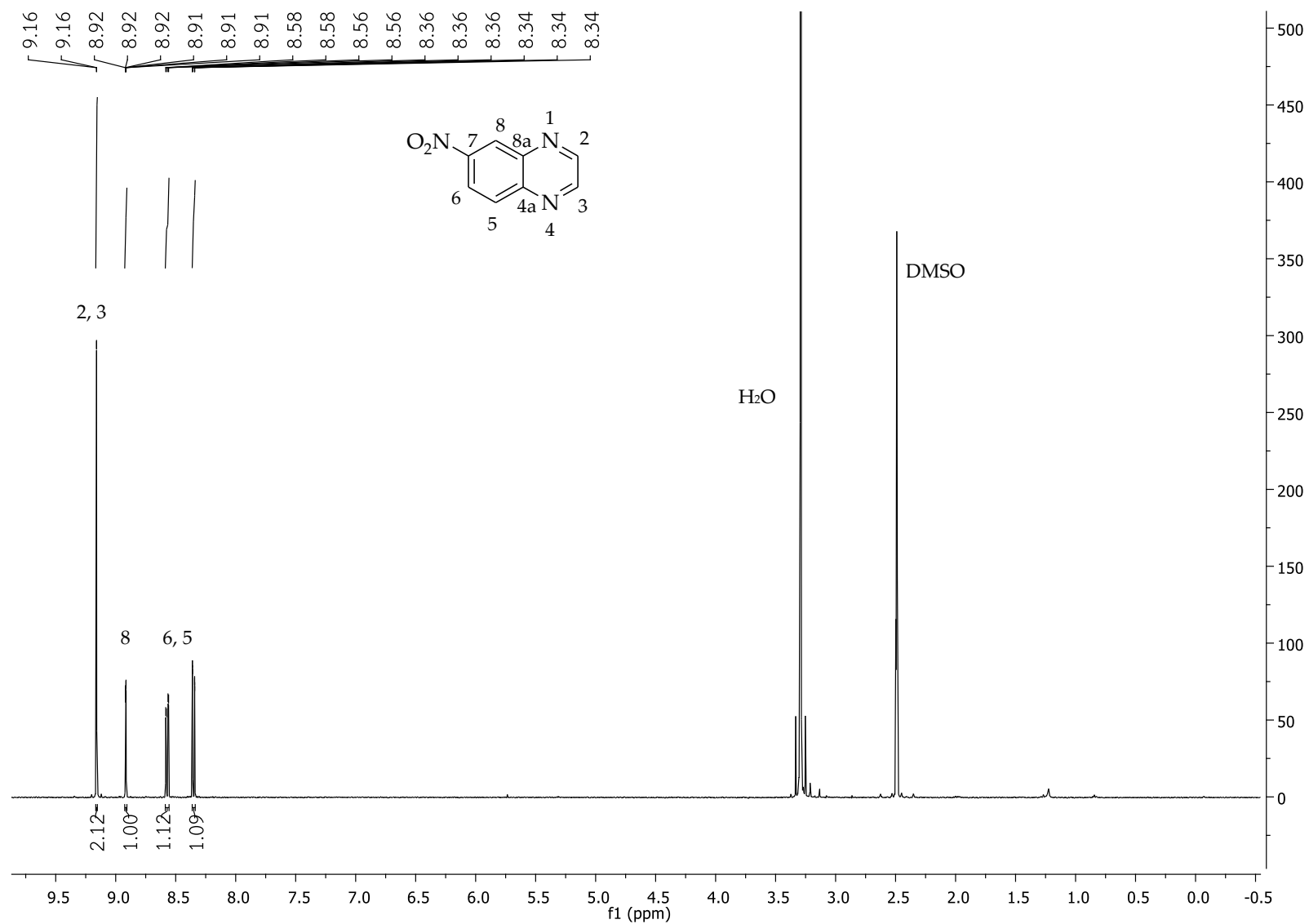


Figure 13. ¹H-NMR spectra of 6-Nitroquinoxaline (5a).

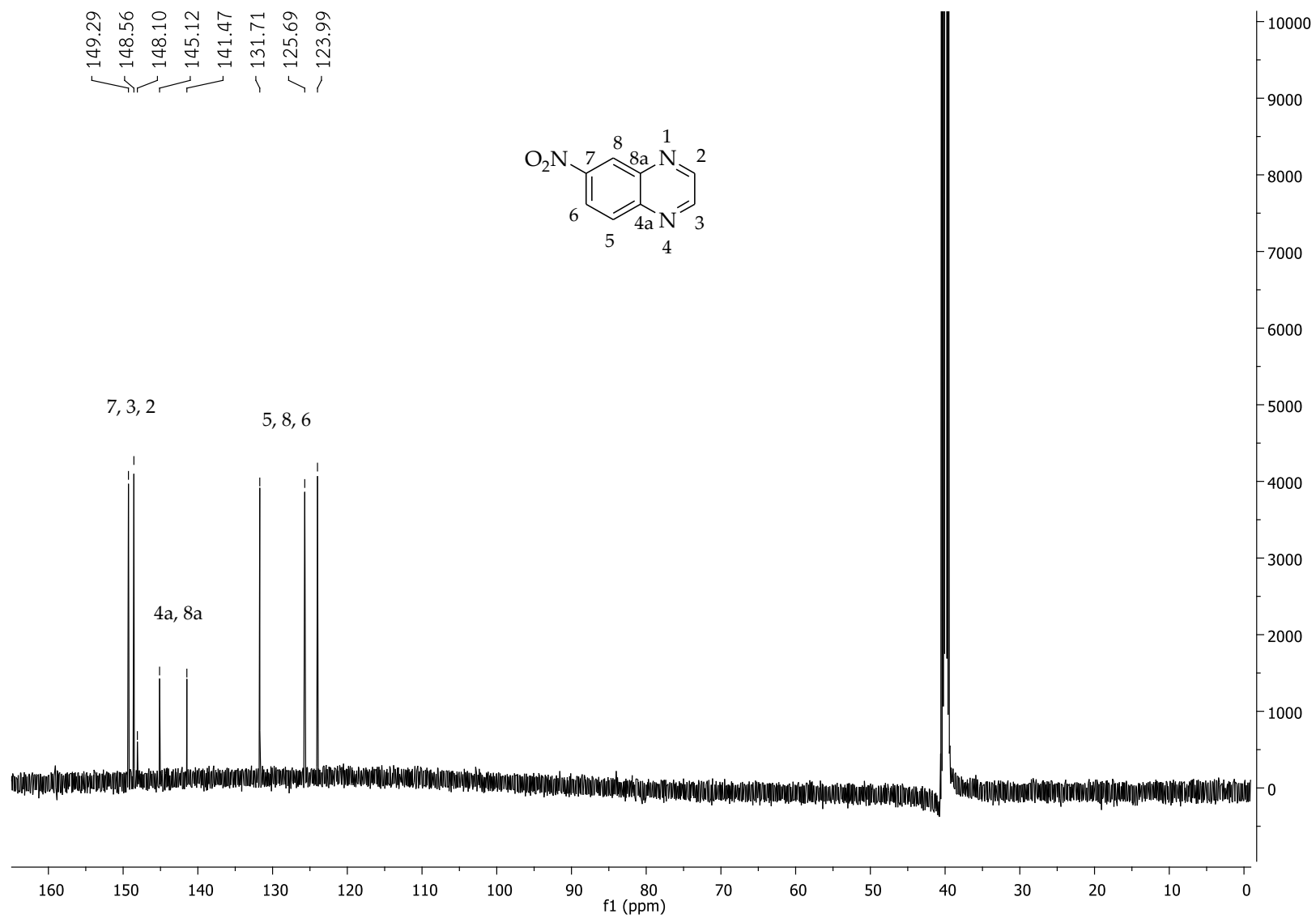


Figure 14. ^{13}C -NMR spectra of 6-Nitroquinoline (5a).

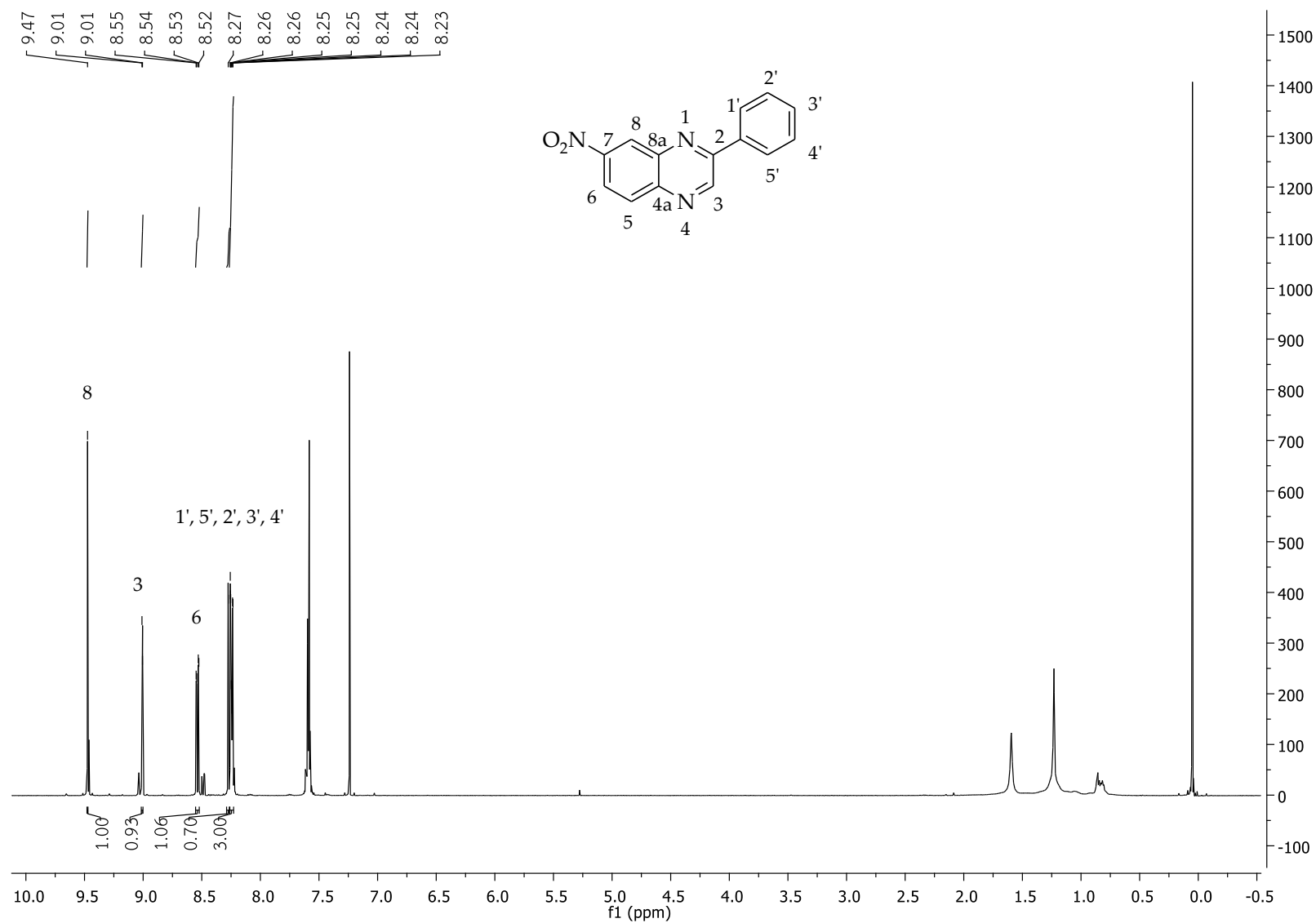


Figure 15. ¹H-NMR spectra of 7-Nitro-2-phenylquinoxaline (**5b**).

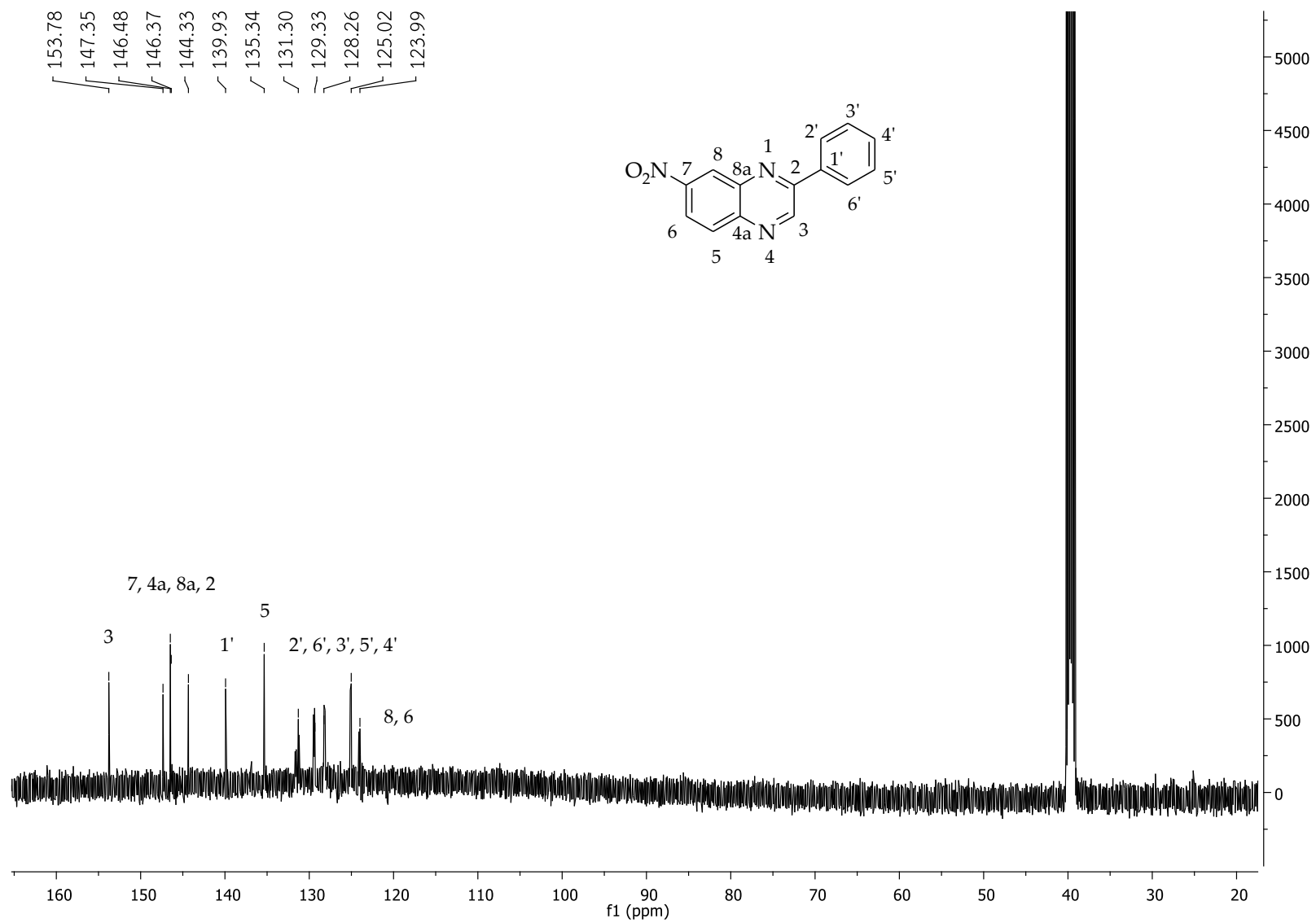


Figure 16. ¹³C-NMR spectra of 7-Nitro-2-phenylquinoxaline (**5b**).

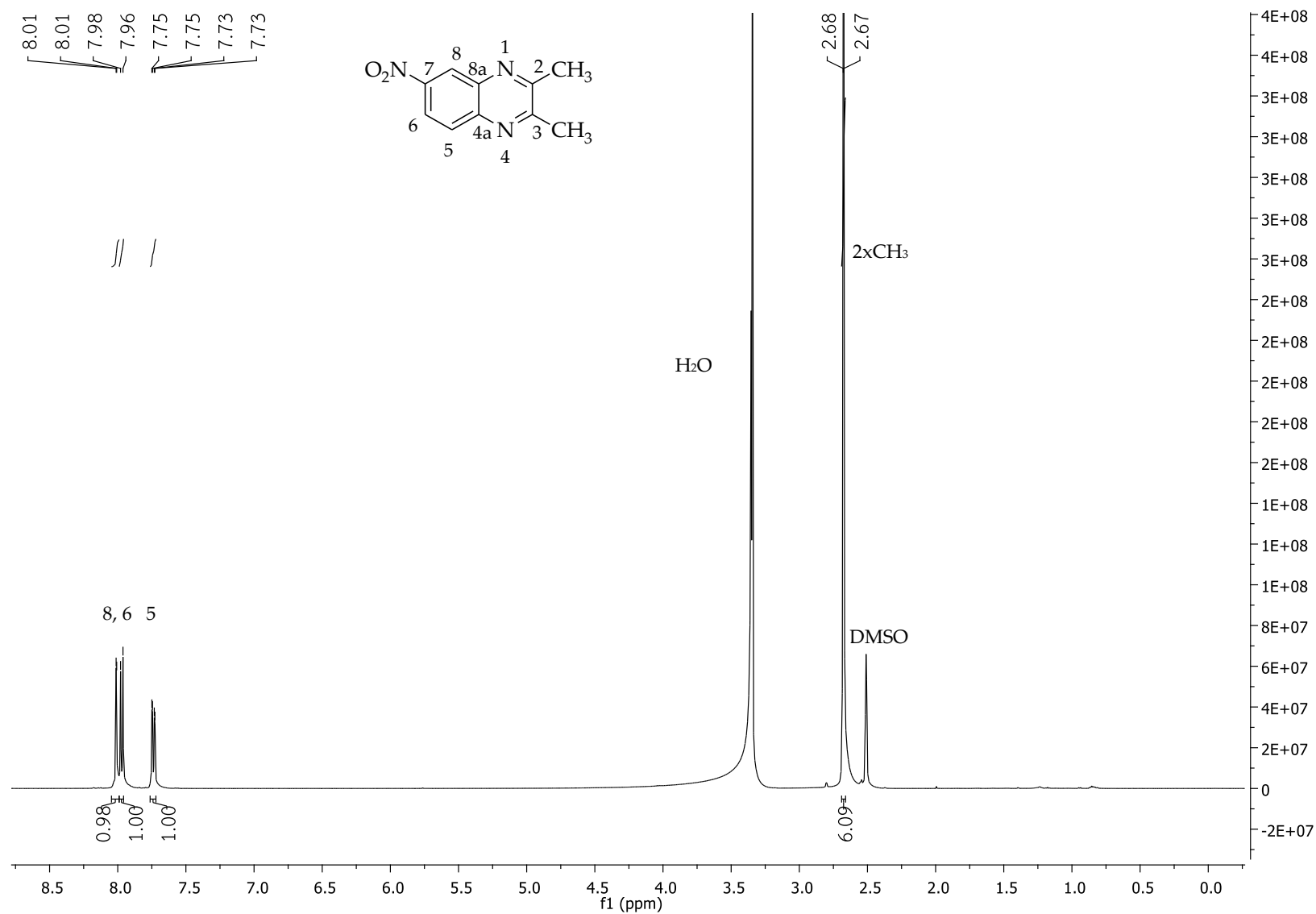


Figure 17. ¹H-NMR spectra of 2,3-Dimethyl-6-nitroquinoxaline (5c).

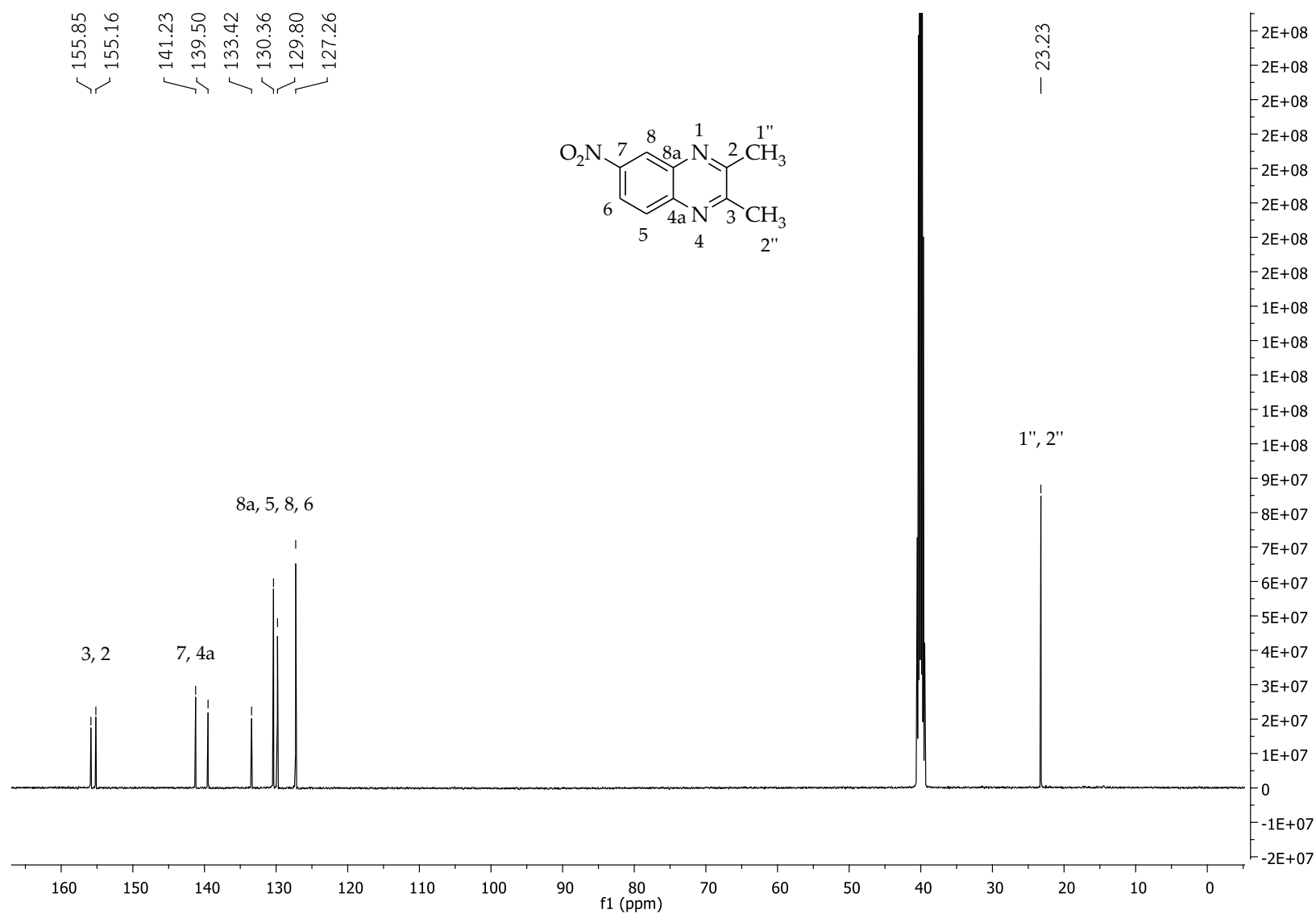


Figure 18. ¹³C-NMR spectra of 2,3-Dimethyl-6-nitroquinoxaline (5c).

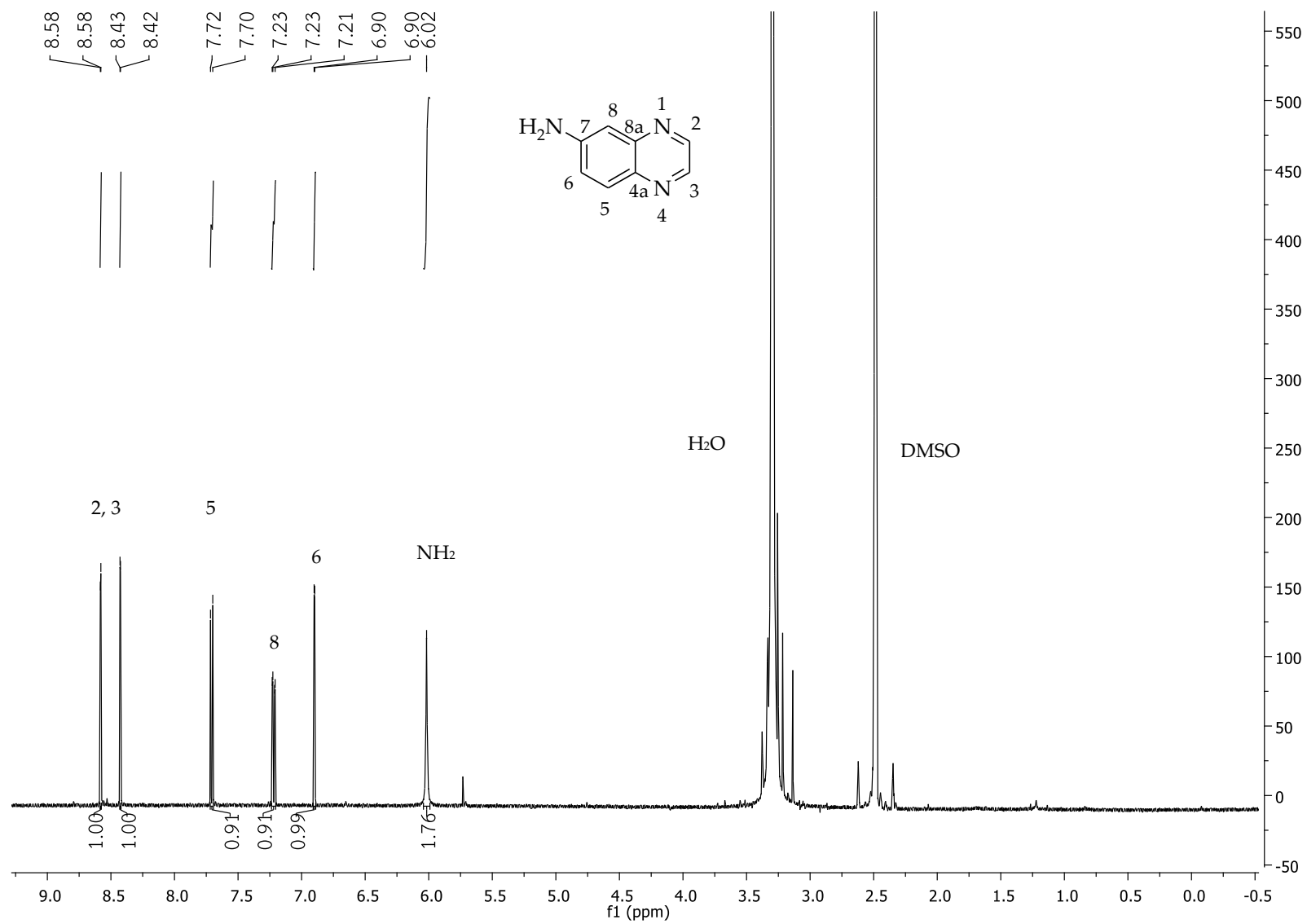


Figure 19. ¹H-NMR spectra of Quinoxalin-6-amine (6a).

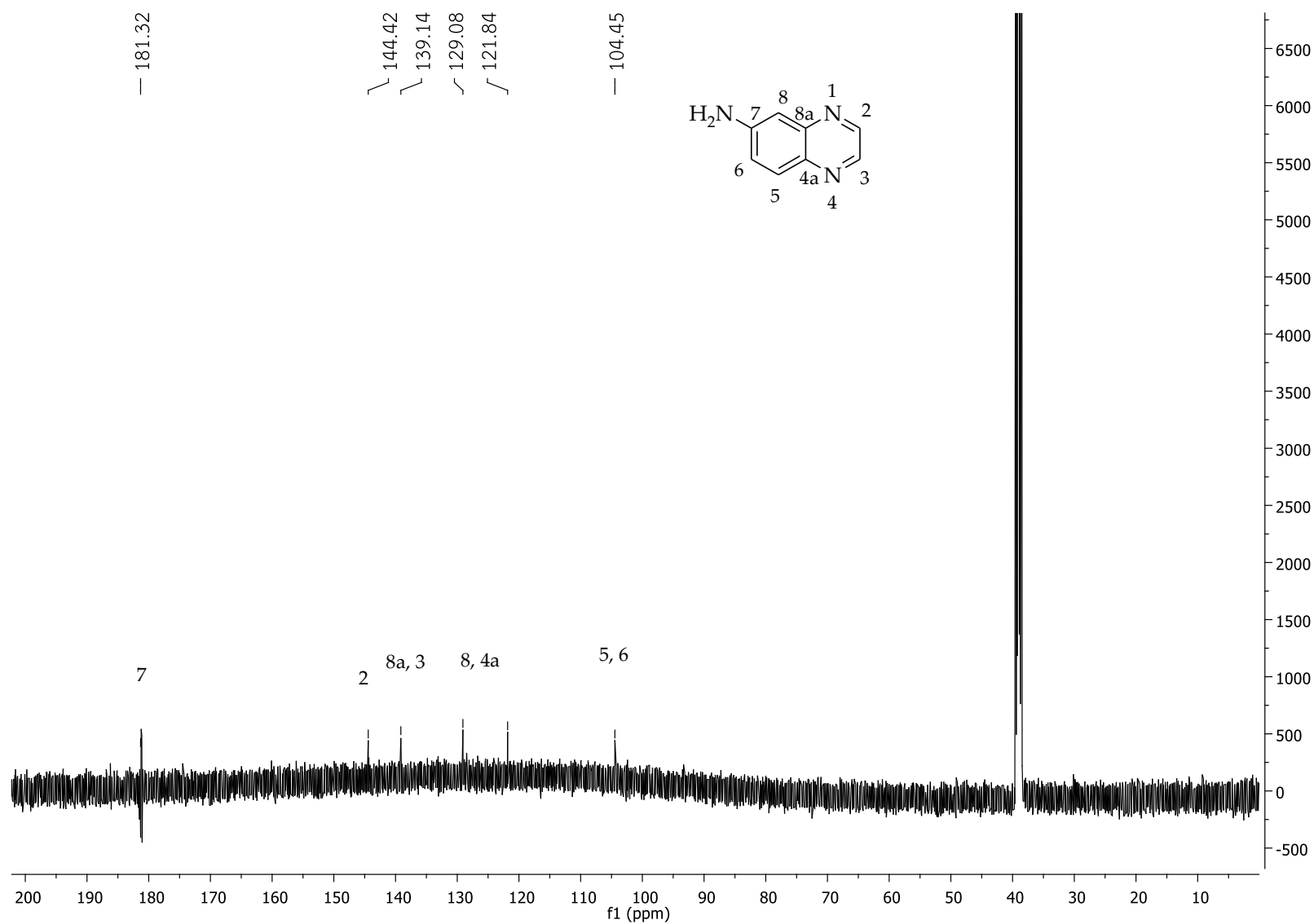


Figure 20. ^{13}C -NMR spectra of Quinoxalin-6-amine (6a).

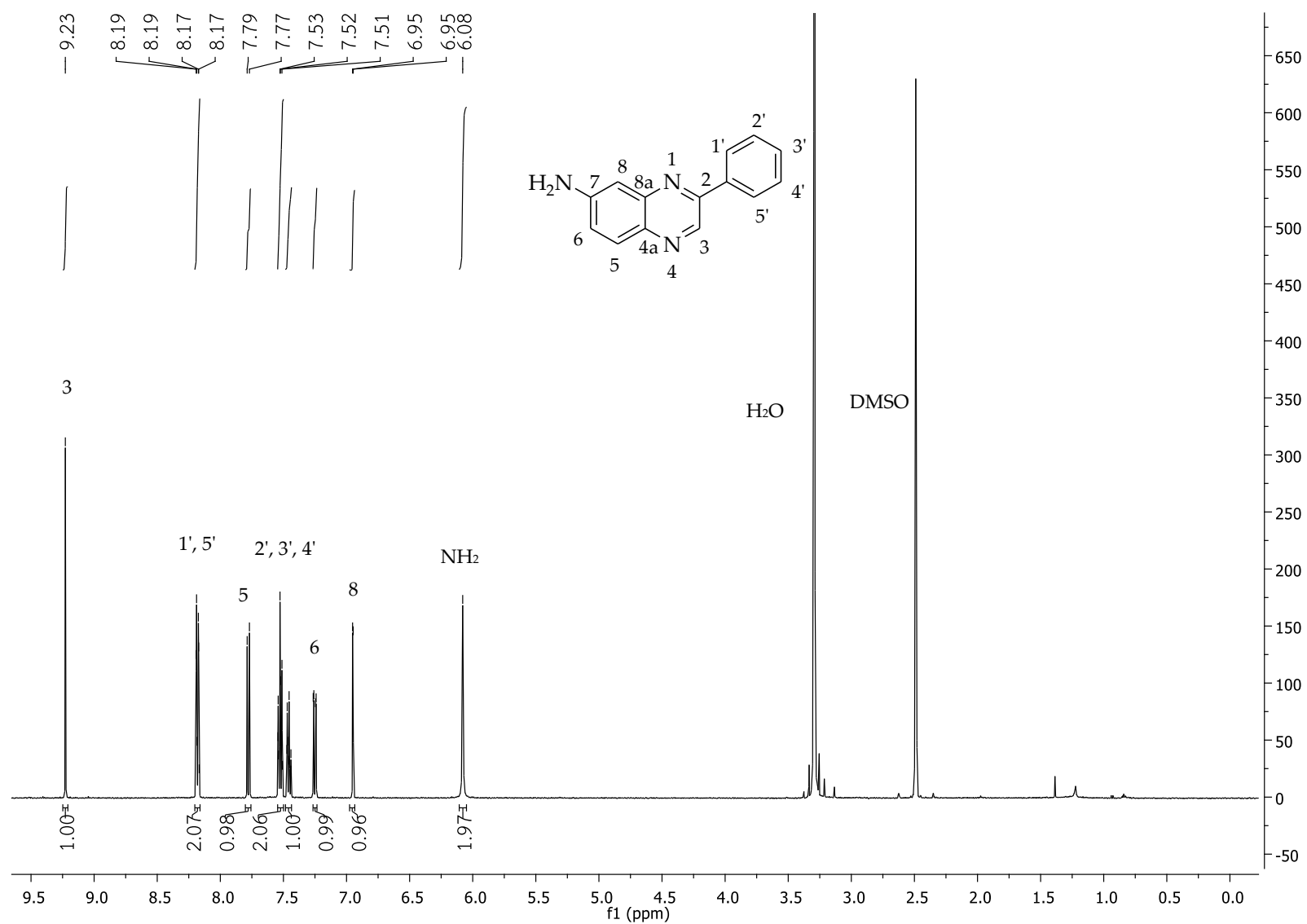


Figure 21. $^1\text{H-NMR}$ spectra of 3-Phenylquinoxalin-6-amine (**6b**).

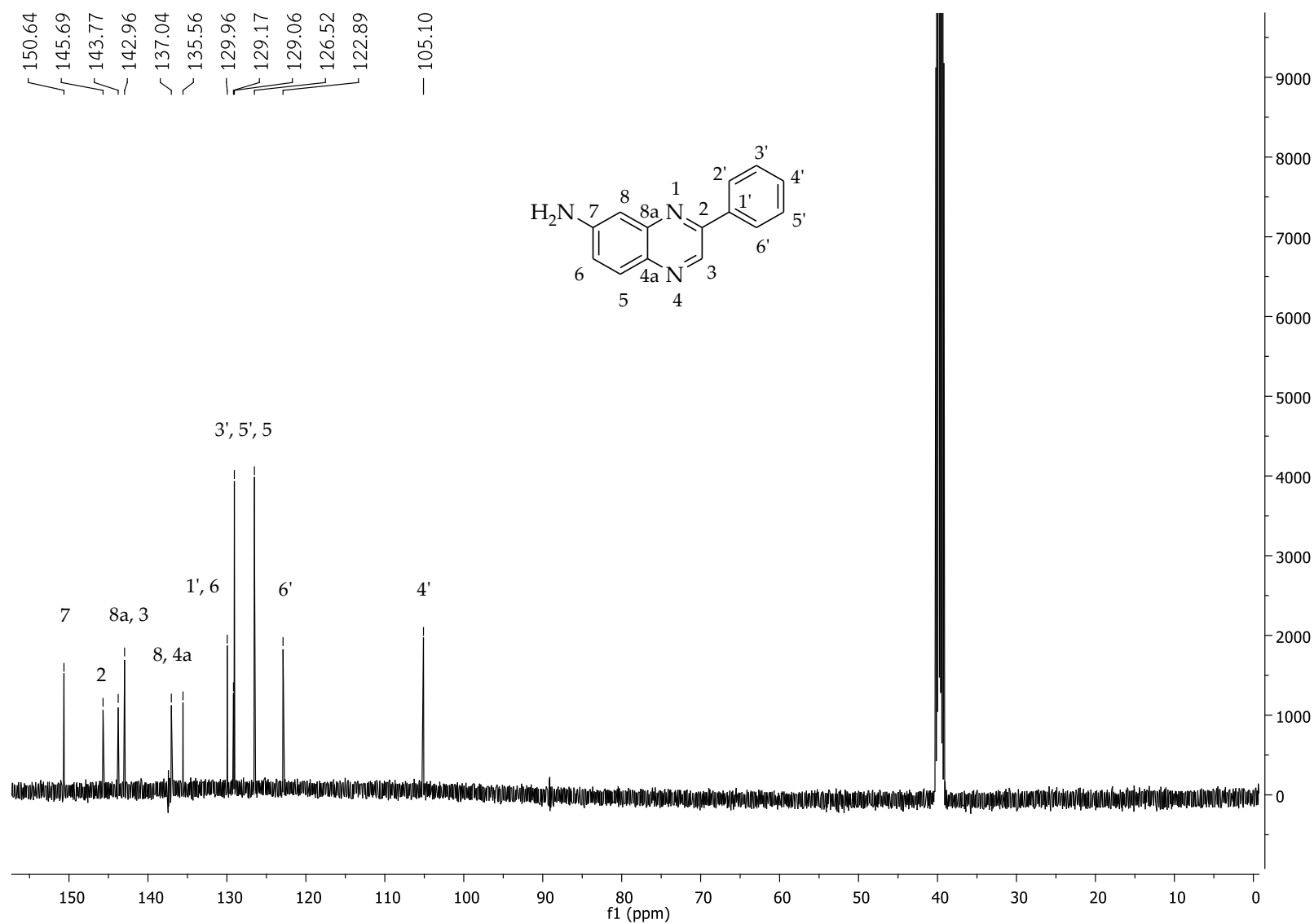


Figure 22. ^{13}C -NMR spectra of 3-Phenylquinoxalin-6-amine (**6b**).

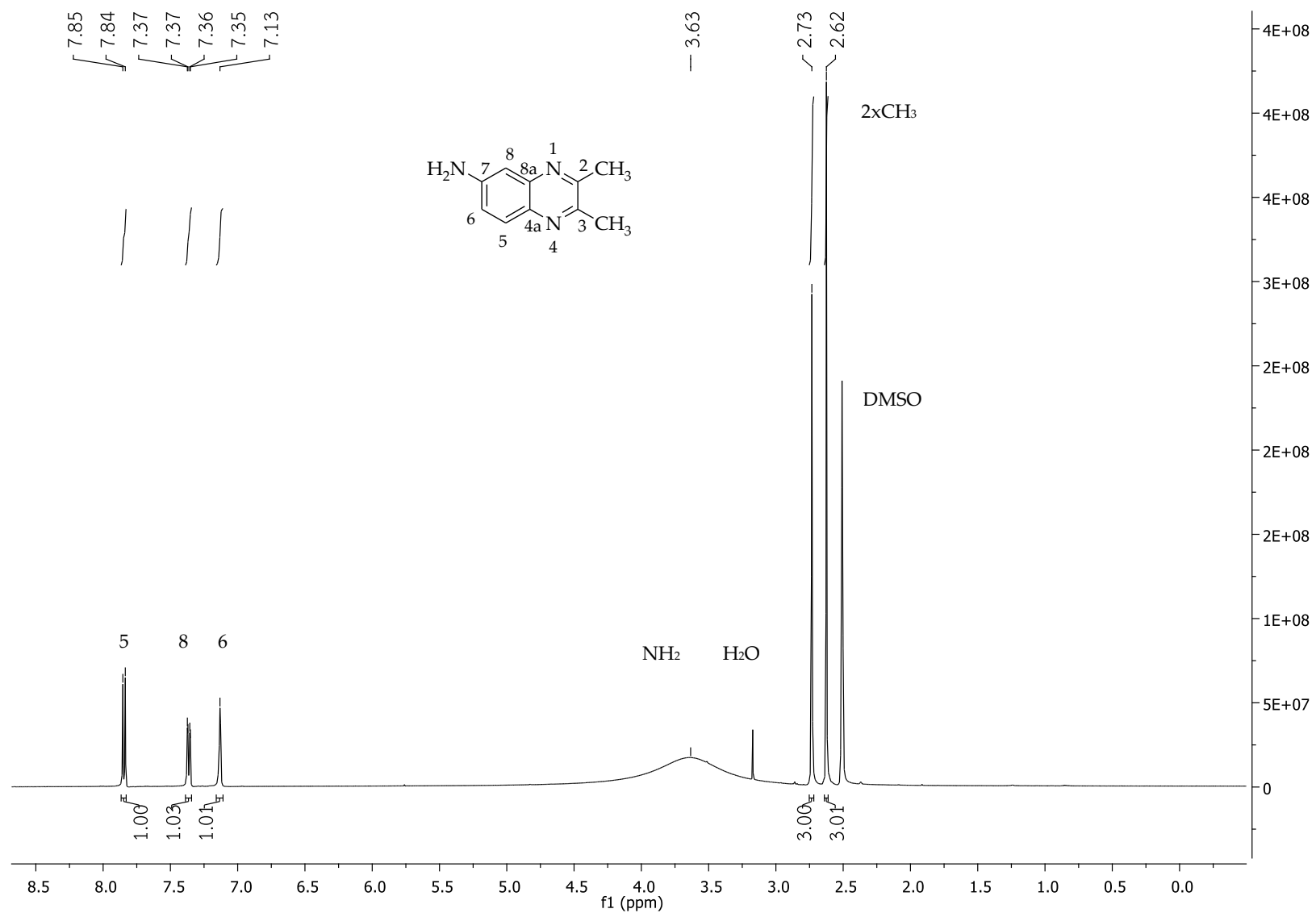


Figure 23. ¹H-NMR spectra of 2,3-Dimethylquinoxalin-6-amine (**6c**).

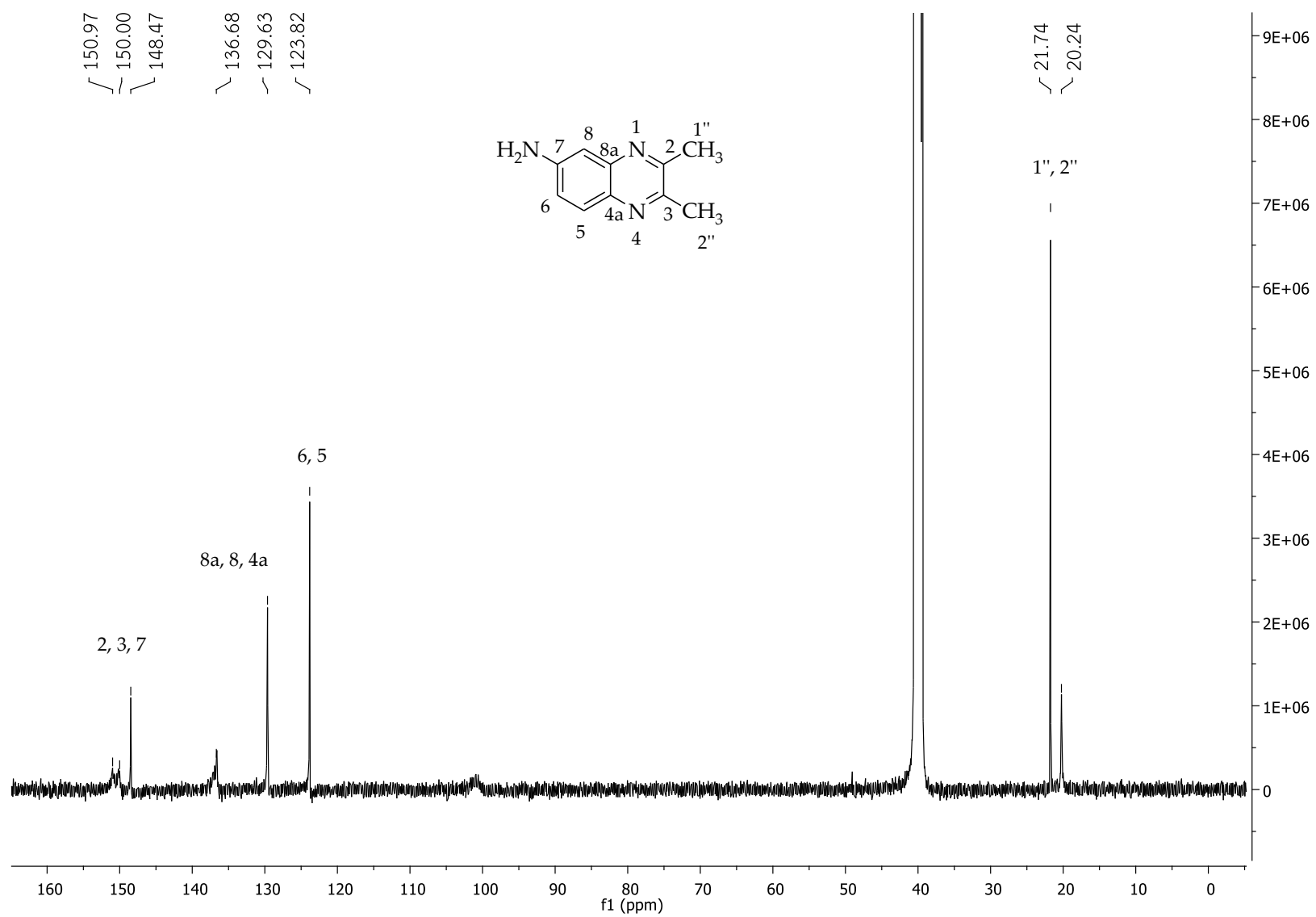


Figure 24. ^{13}C -NMR spectra of 2,3-Dimethylquinoxalin-6-amine (6c).

Parameter: Nonlinear regression, Equation: One site competition

$Y = \text{Bottom} + (\text{Top} - \text{Bottom}) / (1 + 10^{-(X - \text{LogEC}_{50})})$; Competition of radioligand binding to single binding site identified with a radiolabelled ligand.; Enter data with $X = \log(\text{Concentration})$ and $Y = \text{binding}$.

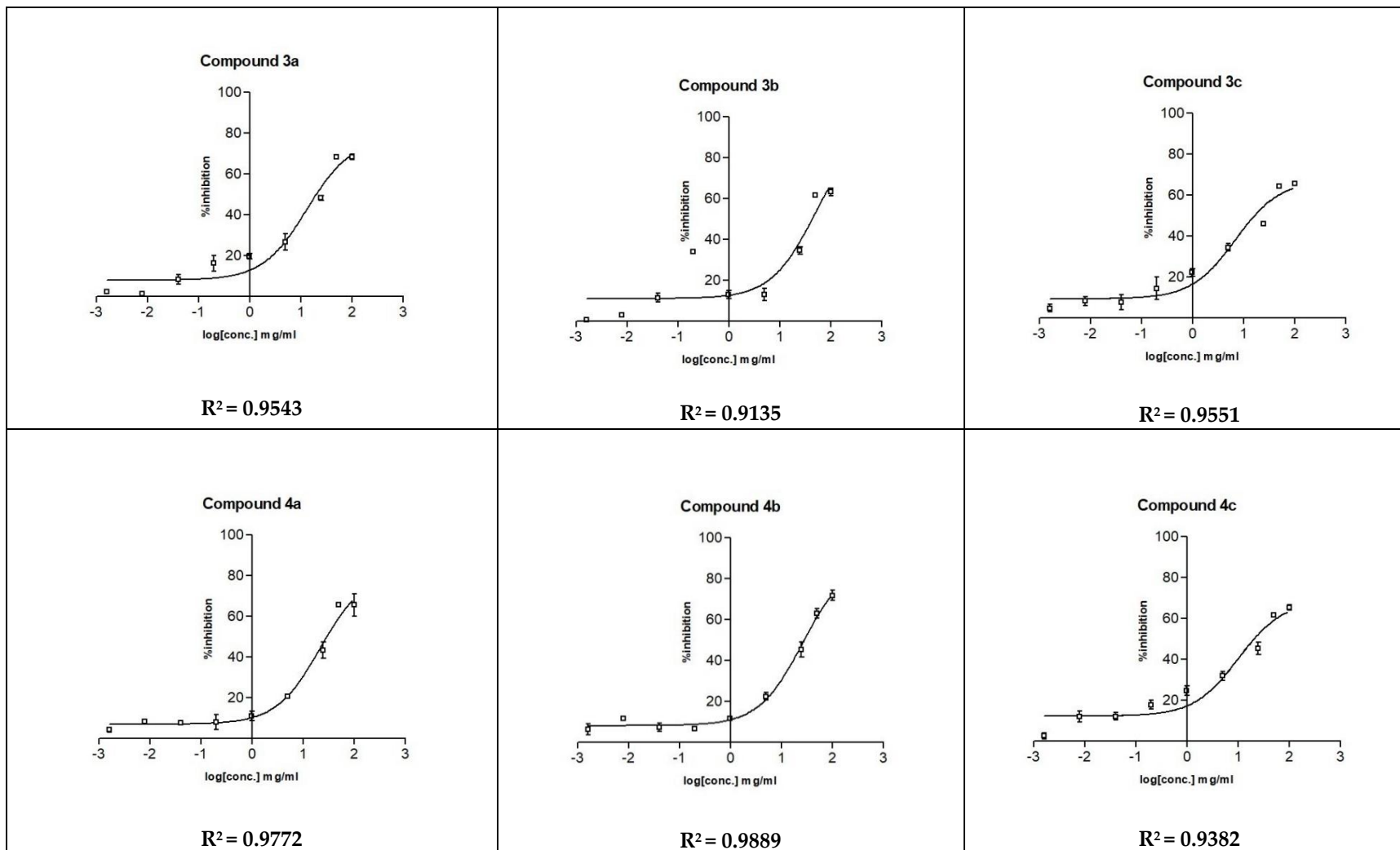


Figure 25. IC₅₀ curves for the inhibition of *HuAChE* by quinoxaline derivatives (3a-4c)

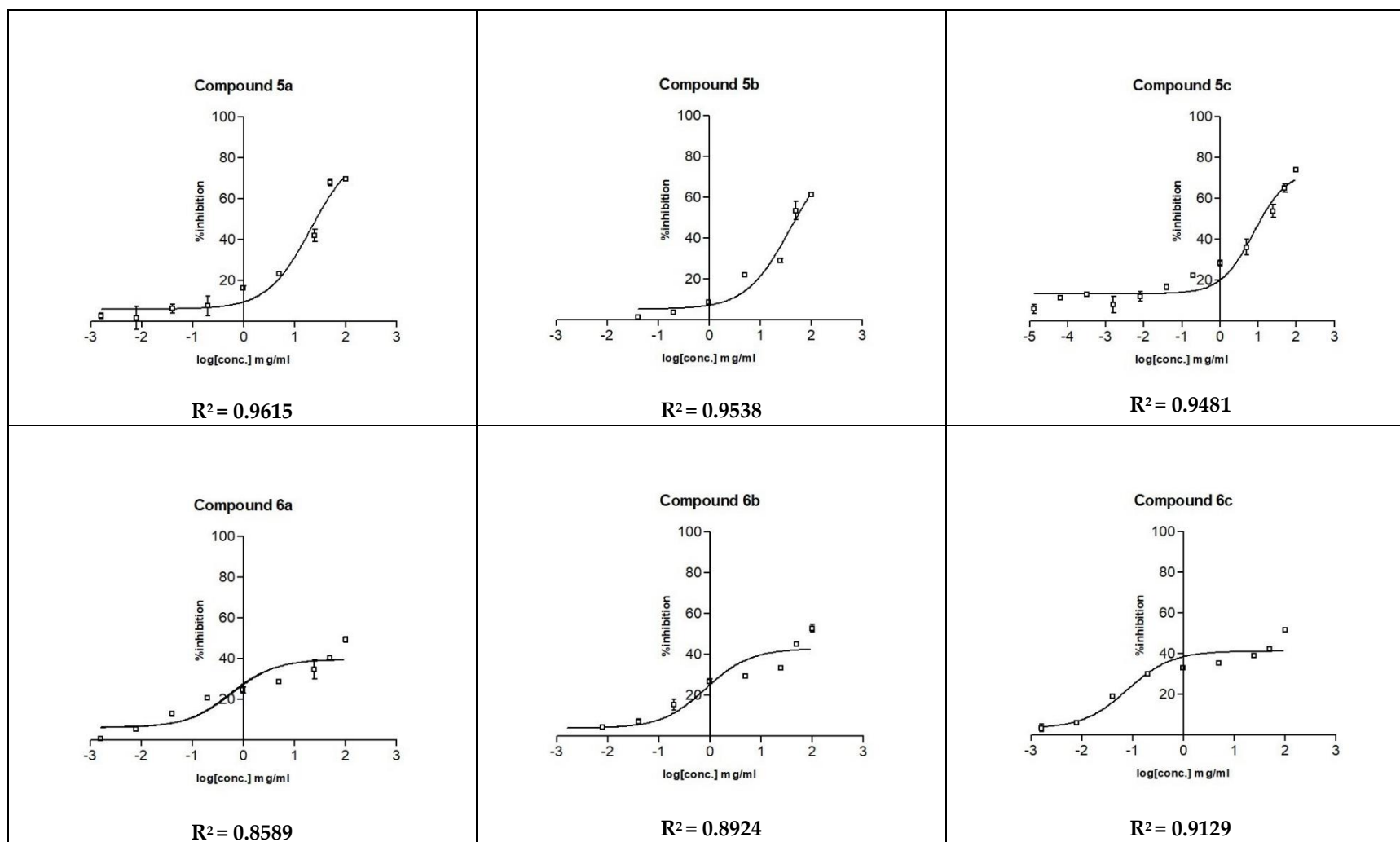
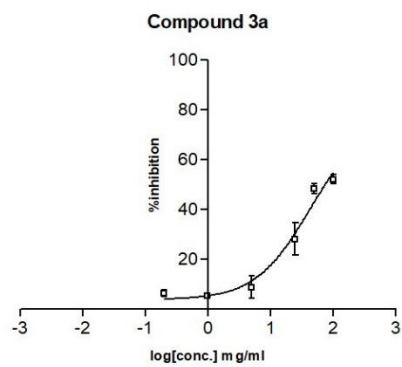
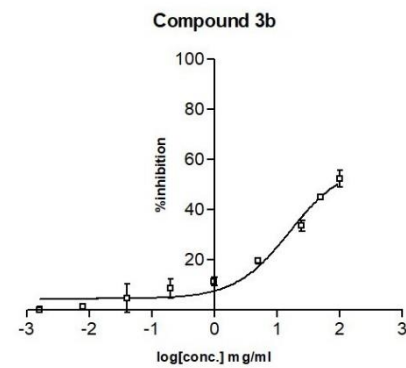


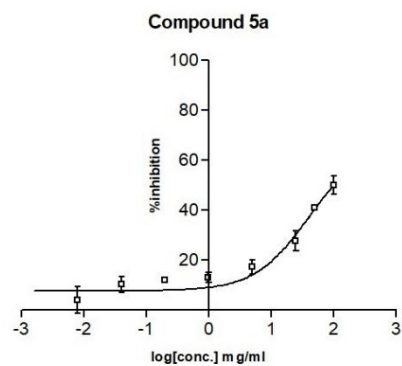
Figure 26. IC₅₀ curves for the inhibition of *HuAChE* by quinoxaline derivatives (5a-6c)



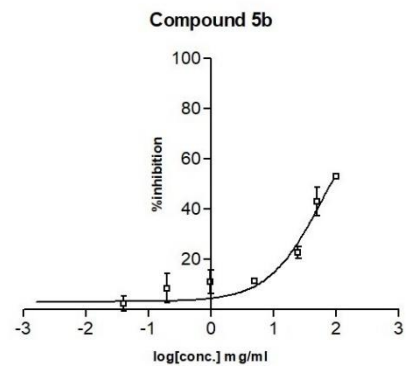
$R^2 = 0.9565$



$R^2 = 0.9603$



$R^2 = 0.9183$



$R^2 = 0.9306$

Figure 27. IC₅₀ curves for the inhibition of *eq*BChE by quinoxaline derivatives (**3a-3b**, **5a-5b**).

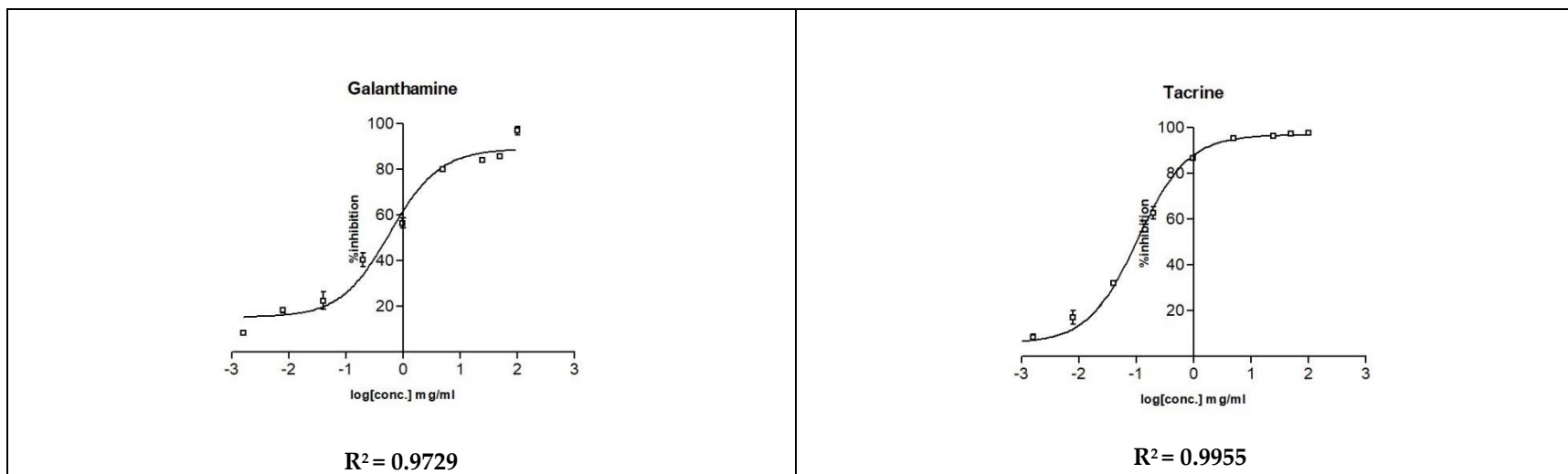


Figure 28. IC₅₀ curves for the inhibition of *HuAChE* by galanthamine and tacrine

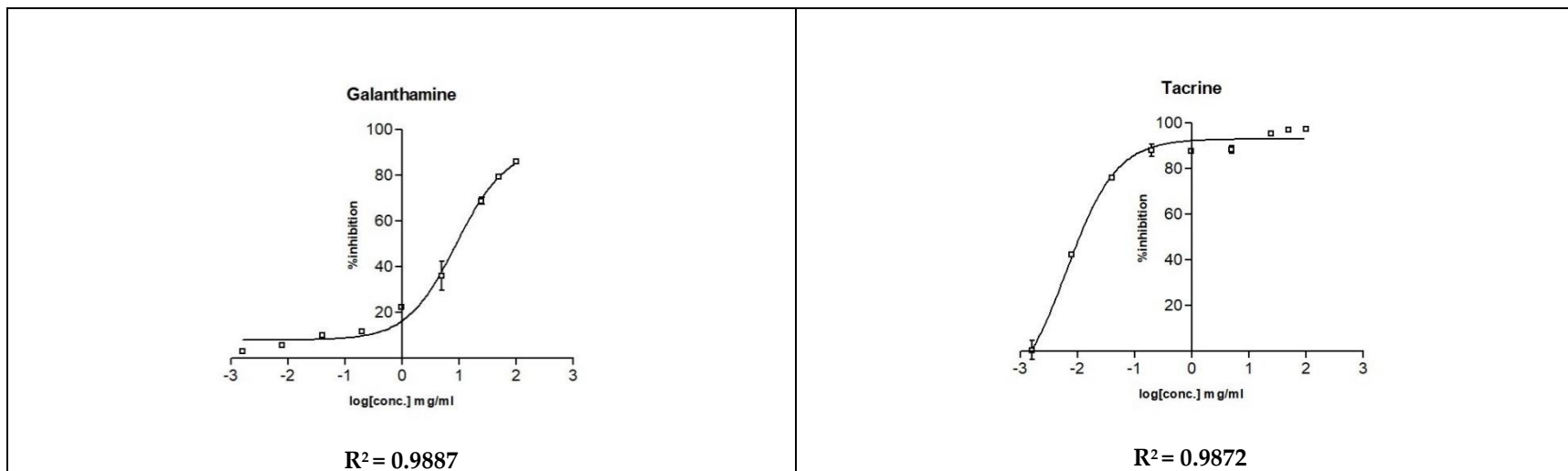
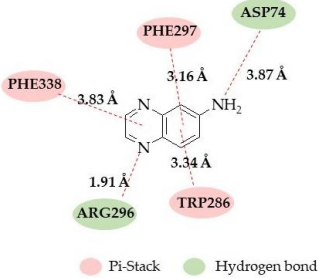
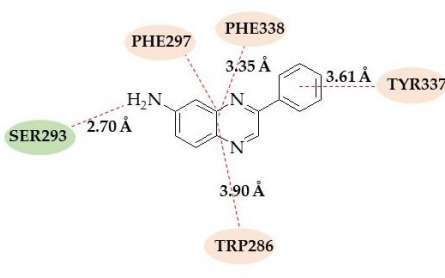
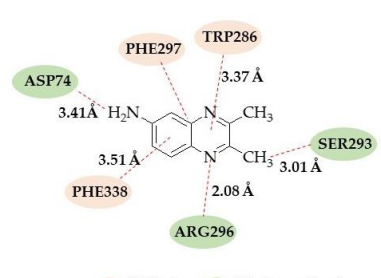
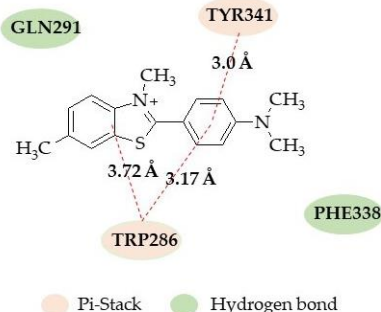
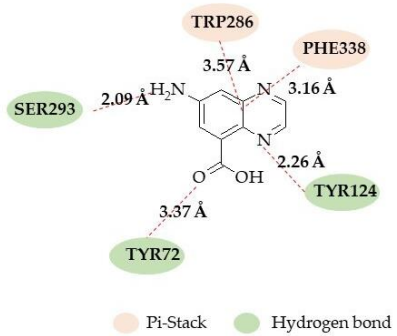
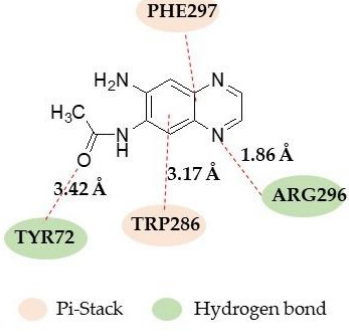


Figure 29. IC₅₀ curves for the inhibition of *eqBChE* by galanthamine and tacrine.

In PAS of active site of *HuAChE* enzyme: 2D schematic diagram of docking model of compounds **6a**, **6b**, **6c** and thioflavinT with *HuAChE*.

Compound 6a	Compound 6b	Compound 6c
		
<p>Compound 6a-<i>HuAChE</i> complex showed affinity of binding energy of -5.68 kcal/mol. The quinoxaline ring can interact with Trp286, Phe297 and Phe338 with π-π interaction and exhibited hydrogen bonding with Asp74 and Arg296.</p>	<p>Compound 6b-<i>HuAChE</i> complex, showed affinity of binding energy of -7.35 kcal/mol. Pyrazine ring of quinoxaline was observed to bind to PAS via a π-π interaction with Trp286, Phe297 and Phe338. Amino group interacted with Ser293 showed hydrogen bond and benzyl group displayed hydrophobic interaction with Tyr337.</p>	<p>compound 6c-<i>HuAChE</i> complex showed affinity of binding energy of -6.32 kcal/mol. Quinoxaline ring showed π-π interaction with Trp286, Phe297 and Phe338. Nitrogen atom of the pyrazine ring showed hydrogen bond with Arg296. Amino group interacted with Asp74 via hydrogen bond. Methyl group displayed hydrogen bond with Ser293.</p>
ThioflavinT		
		
<p>Thioflavin T-<i>HuAChE</i> complex, showed affinity of binding energy of -8.29 kcal/mol. Benzothiazol ring was observed to bind to PAS via a π-π interaction with Trp286. Benzyl group displayed π-π interaction with Trp286 and Tyr341.</p>		

In the area of PAS of *HuAChE*, (a) 3D docking model of compound 27 complex with *HuAChE*. (b) 3D docking of compound 21 complex with *HuAChE*.

(a): Compound 27	(b): Compound 21
	
Binding Energy: -4.80 kcal/mol	Binding Energy: -7.13 kcal/mol
<p>Compound 27-<i>HuAChE</i> complex (a), The quinoxaline ring showed π-π stack interaction with Trp286 and Phe338. Nitrogen atom of pyrazine ring formed hydrogen bond with Tyr124. Amino group on quinoxaline ring exhibited hydrogen bond with Ser293 and carboxylic group displayed hydrogen bond with Tyr72.</p>	<p>Compound 21-<i>HuAChE</i> complex (b), the quinoxaline ring showed π-π stack interaction with Trp286 and Phe297. The nitrogen atom of the pyrazine ring showed hydrogen bond with Arg296. Carbonyl group on quinoxaline ring exhibited hydrogen bond with Tyr72.</p>